Functional analysis of the *Nematostella* Wnt/β-catenin destruction complex provides insight into the evolution of a critical regulatory module in a major metazoan signal transduction pathway

Authors: Hongyan Sun[1,†], Brian M. Walters[1], Radim Zidek[2], Mark Q. Martindale[2] and Athula H. Wikramanayake[1*]

Affiliations:

[1]Department of Biology, University of Miami, Coral Gables, FL, 33146

[2]Whitney Laboratory for Marine Bioscience, 9505 Ocean Shore Blvd. St. Augustine, FL 32080-8610

[†] Current address: Pennington Biomedical Research Center, Baton Rouge, LA, 70808

[*]Corresponding author (athula@miami.edu)

Key Words: Wnt/β-catenin signaling, Axin, Adenomatous Polyposis Coli, evolution of signal transduction pathways, Wnt/β-catenin destruction complex, *Nematostella*, Cnidaria, Mnemiopsis, Ctenophora

Abstract

The genesis of signaling pathways likely drove metazoan evolution, but the origins of these pathways and how they acquired signaling activity is poorly understood. Here, we studied functional evolution of the Wnt/β-catenin (cWnt) pathway destruction-complex (DC) that regulates β-catenin signaling. Bilaterian DC function requires β-catenin binding to Axin and APC proteins, and Axin-APC heterodimerization. However, bioinformatic analyses predicted that Axin and APC-like homologs in early-branching non-bilaterians lack important previously defined bilaterian β-catenin binding domains, questioning if they have functional cWnt-DCs. We demonstrate that both Axin and APC proteins in the cnidarian *Nematostella vectensis* (a representative of the sister taxon to bilaterians) can regulate cWnt signaling indicating an active cWnt-DC. Using *in vitro* analyses, we show that NvAxin binds Nvβ-catenin weakly despite lacking the conserved bilaterian Axin β-catenin-binding motif (βcatBM). Using AlphaFold3, we identified two predicted βcatBM-like sequences in NvAxin, one within the Axin-RGS domain and another towards the C-terminus. Similar analysis of placozoan, poriferan, and ctenophore Axin identified single βcatBM-like sequences located within Axin-RGS. We show that ctenophore Axin and β-catenin do not interact and changing a conserved leucine on NvAxin-βcatBM-like motifs to resemble the ctenophore sequence abolished NvAxin-Nvβ-catenin interactions. We propose that an ancestral Axin-RGS sequence acquired low-affinity β-catenin binding early in metazoan evolution, followed by motif duplication in the cnidarian-bilaterian ancestor. In bilaterians, the duplicated βcatBM evolved higher-affinity for β-catenin, while the ancestral sequence was lost. Our results demonstrate how phylogenetic insights, AI tools and functional assays can be used to reconstruct the evolution of complex signaling pathways.

48 **Introduction**

49 The early development and diversification of multicellular animals (metazoans) is
50 regulated by a small set of conserved signal transduction pathways (Gerhart 1999; Pires-
51 daSilva and Sommer 2003; Richards and Degnan 2009; Babonis and Martindale 2017).
52 It has been hypothesized that the evolution of these signaling pathways was critical for
53 the evolution and radiation of the metazoan last common ancestor, or "urmetazoan",
54 over 600 million years ago (Pires-daSilva and Sommer 2003; Rokas 2008; Richards and
55 Degnan 2009; Babonis & Martindale, 2017; Richter and King 2013; Ros-Rocher et al.
56 2021). Despite the critical roles of these pathways in metazoan development and
57 evolution, relatively little is known about their origins or their functional activity in early
58 emerging taxa (Pires-daSilva and Sommer 2003; Babonis & Martindale, 2017; Richards
59 and Degnan 2009). One major constraint to advancing this research has been the
60 difficulty in the care and handling of embryos of early emerging (non-bilaterian) model
61 systems to experimentally manipulate signal transduction pathways. However, the
62 advancement of methodology to molecularly manipulate development in cnidarians
63 (e.g., sea anemones, corals, "jelly fish"), the closest outgroup to the Bilateria (Fig. 1A),
64 and foundational knowledge of Wnt/β-catenin (cWnt) pathway function in these
65 animals and has established cnidarians as one of the best non-bilaterian experimental
66 systems to functionally understand the direction of evolutionary change in the cWnt
67 signaling pathway (Wikramanayake et al. 2003; Lee et al. 2007; Layden et al. 2016;
68 Lebedeva et al. 2021; Houliston et al. 2022; Holzem et al. 2024).

69 The cWnt signaling pathway (Fig. 1B) is a broadly deployed signaling pathway
70 that is restricted to the Metazoa, and cWnt signaling plays diverse roles during
71 evolution, development and homeostasis (Petersen and Reddien 2009; Richards and

72 Degnan 2009; Loh et al. 2016; Babonis and Martindale 2017; Richter et al. 2018;
73 Holzem et al. 2024). Extensive studies of cWnt pathway function in bilaterian models
74 have led to a relatively advanced level of understanding of the critical regulatory nodes
75 in this pathway, hence making it a particularly useful model to investigate how
76 metazoan signaling pathways evolved and acquired signaling competence. For example,
77 like many of the metazoan signal transduction pathways, the cWnt pathway is modular
78 in its organization, with distinct protein complexes regulating transduction of signals
79 from the cell surface to the nucleus (MacDonald et al. 2009; Stamos and Weis 2013;
80 Gammons and Bienz 2018; Liu et al. 2022). One critical cytoplasmic regulatory node in
81 the cWnt pathway is the β-catenin destruction complex (DC) which is essential for
82 regulating cWnt signaling through the control of cytoplasmic levels of β-catenin, the
83 primary transducer of cWnt signaling in the nucleus (Fig. 1B) (Roberts et al. 2011;
84 Stamos and Weis 2013; Gammons and Bienz 2018). Evolution of the DC was critical for
85 the evolution of cWnt signaling because it likely provided a scaffold for exaptation of β-
86 catenin for a signaling function. Moreover, the DC also may have provided a central
87 regulatory node for context-dependent spatial and temporal control of this pathway
88 during its wide deployment in bilaterians during development and homeostasis
89 (Petersen and Reddien 2009; Valenta et al. 2012; Loh et al. 2016; Liu et al. 2022;
90 Holzem et al. 2024).

91 Axin is a key scaffolding protein in the bilaterian DC which contains multiple
92 binding sites that mediate its direct association with proteins in the DC including β-
93 catenin, the two serine/threonine protein kinases Casein Kinase 1α (CK-1α) and
94 Glycogen Synthase Kinase 3β (GSK-3β), the phosphoprotein Disheveled (Dvl), and APC,
95 the product of the Adenomatous Polyposis Coli gene (Fig. 1C) (Ikeda et al. 1998; Kishida

96 et al. 1998; Fagotto et al. 1999; Valenta et al. 2012; Stamos and Weis 2013; Pronobis et
97 al. 2015; van Kappel and Maurice 2017; Qiu et al. 2024). A detailed model for negative
98 regulation of β-catenin in the cWnt pathway by the DC has emerged from extensive
99 functional studies done in vertebrate and invertebrate model systems (Roberts et al.
100 2011; Stamos and Weis 2013; van Kappel and Maurice 2017; Liu et al. 2022; Kremer et
101 al. 2010; Peterson-Nedry et al. 2008). This model proposes that β-catenin is recruited
102 to Axin through a conserved binding motif (βcatBM) and this binding mediates the
103 sequential phosphorylation of β-catenin by CK-1α and GSK-3β leading to its
104 ubiquitylation and proteasome-mediated degradation (Xing et al. 2003; Kimelman and
105 Xu 2006; Roberts et al. 2011; Stamos and Weis 2013; van Kappel and Maurice 2017;
106 Gammons and Bienz 2018; Ranes et al. 2021). The transfer of phosphorylated β-catenin
107 to the proteasome requires APC, the second scaffolding protein in the DC. APC in
108 bilaterians is a relatively large protein with multiple domains that have been shown to
109 mediate its interactions with Axin, β-catenin, and over 100 other proteins (Fig. 1D)
110 (Roberts et al. 2011; Nelson and Näthke 2013; van Kappel and Maurice 2017; Abbott
111 and Näthke 2023). Strikingly, APC has multiple distinct binding sites for β-catenin that
112 have different affinities for the protein (Ha et al. 2004; Kimelman and Xu 2006;
113 Roberts et al. 2011; Pronobis et al. 2017; Ranes et al. 2021). Current models postulate
114 that following β-catenin phosphorylation on Axin, one of the 20 amino acid repeats on
115 APC is phosphorylated and subsequently phosphorylated β-catenin is transferred to this
116 domain on APC prior to being targeted to the proteasome for degradation (Kimelman &
117 Xu, 2006; Roberts et al. 2011; Ranes et al. 2021). Regulation of the DC has been subject
118 to extensive experimental interrogation because of its critical role in regulating cWnt
119 signaling, and the discovery that over 90% of human colorectal cancers have mutations

120 in either APC or other components of the DC that can lead to misregulation of cWnt
121 signaling (Polakis 1995; Kinzler and Vogelstein 1996; Fodde et al. 2001; Schneikert and
122 Behrens 2007; Kohler et al. 2008). Oncogenic human APC mutations are frequently
123 seen in the "mutational cluster region" (MCR) that delete many of the well-characterized
124 β-catenin binding sites and the three SAMP domains on the protein that mediate Axin-
125 APC heterodimerization and are required for DC function (Fig. 1D) (Kinzler and
126 Vogelstein 1996; Fodde et al. 2001; Schneikert and Behrens 2007; Kohler et al. 2008;
127 Roberts et al. 2011; Ranes et al. 2021).

128 The cWnt pathway is deeply conserved with homologs of components of the basic
129 pathway found in all metazoan phyla (Richards and Degnan 2009; Babonis and
130 Martindale 2017; Holzem et al. 2024), but ongoing genomic sequencing studies in early
131 branching metazoan clades have raised interesting fundamental questions about the
132 origin of signaling competence in the cWnt pathway. One of the first observations that
133 raised the possibility that the non-bilaterian cWnt pathway may not function like the
134 bilaterian cWnt pathway came from a phylogenetic analysis of Wnt pathway
135 components in two early emerging taxa, the poriferan (sponge) *Amphimedon*
136 *queenslandica* and the cnidarian (sea anemone) *Nematostella vectensis* (Richards and
137 Degnan, 2009; Adamska et al. 2010). This work showed that protein domains known to
138 be important in DC proteins in bilaterians were absent in these two species. For
139 example, the Axin proteins from *A. queenslandica* and *N. vectensis* appeared to lack the
140 highly conserved βcatBM seen in bilaterian Axin that mediates its interaction with β-
141 catenin (Richards and Degnan 2009; Adamska et al. 2010) (Fig. 1C). We used the
142 webtool SMART (Simple Modular Architecture Research Tool: http://smart.embl-
143 heidelberg.de) to confirm that Axin from a ctenophore and a placozoan also lack the

144 βcatBM suggesting its bilaterian origin (Fig. 1C). Additionally, APC proteins in these
145 taxa were considerably shorter than the bilaterian homologs, lacking many of the critical
146 protein-protein interaction domains seen in bilaterians (Richards and Degnan 2009;
147 Adamska et al. 2010) (Fig. 1D), and the corresponding genes have recently been
148 classified as "*APC-like*" (Adamska et al. 2010; Abbott and Näthke 2023) suggested that
149 the Axin and APC-like proteins in these early diverging taxa may not be part of the DC,
150 or that these proteins may be interacting in different ways to regulate DC function.
151 These observations provided a fundamental opportunity to better understand the
152 evolution of the regulation of a major metazoan signaling pathway and to reconstruct
153 the ancestral state of a critical regulatory node in the cnidarian-bilaterian last common
154 ancestor (LCA).

155 In this study we carried out a detailed functional analysis of the cWnt DC in the
156 cnidarian *Nematostella* to determine how it functions in the absence of critical domains
157 in Axin and APC required for bilaterian DC function. We show that *Nematostella* Axin
158 and APC-like proteins use novel protein-protein interactions to form a cWnt DC
159 suggesting that these proteins may have a level of promiscuity not reported in the
160 bilaterian cWnt DC. Additionally, using *in vitro* and *in vivo* protein-protein interaction
161 assays along with AI-enabled prediction we trace the evolutionary history of the critical
162 βcatBM on the bilaterian Axin protein from pre-bilaterian antecedents. We functionally
163 validate the regulation of a non-bilaterian DC function showing that cWnt signaling can
164 achieve deeply conserved developmental outcomes despite significant differences in the
165 regulation of the DC compared to bilaterians. Our results indicate that the key
166 scaffolding proteins in the cWnt DC in the cnidarian-bilaterian last common ancestor
167 were "promiscuous" which provides insight into the mechanisms leading to the

168 evolvability of the signaling pathways in bilaterians promoting the genesis of novel body
169 plans.
170
171 **Results**
172 ***The conserved β-catenin binding motif in bilaterian Axin proteins is not***
173 ***detectable in non-bilaterian Axins***
174 Structure-function studies in bilaterians have defined conserved regions on the
175 Axin protein that allow it to bind to APC, GSK-3β, and β-catenin in the DC thereby
176 promoting β-catenin phosphorylation and targeting it for degradation, maintaining the
177 pathway in an inactive state (Ikeda et al. 1998; Kishida et al. 1998; Fagotto et al. 1999;
178 Valenta et al. 2012; Stamos and Weis 2013; Pronobis et al. 2015; van Kappel and
179 Maurice 2017; Qiu et al. 2024) (Fig. 1C; Supplementary Table 1). In addition, Axin
180 proteins have a defined domain that binds to "activated" Disheveled when the cWnt
181 pathway is stimulated by upstream signals and a more poorly defined region that
182 interacts with CK-1α (Liu et al. 2002; MacDonald et al. 2009; Gammons and Bienz
183 2018; Qiu et al. 2024) (Fig. 1C; Supplementary Table 1). These Axin domains play a
184 critical role in recruiting components of the DC to regulate β-catenin stability (Xing et
185 al. 2003; Mendoza-Topaz et al. 2011; Stamos and Weis 2013; Qiu et al. 2024). A
186 previous bioinformatic analysis showed that the βcatBM is absent in *Amphimedon*
187 (Porifera) and *Nematostella* (Cnidaria) Axin proteins (Adamska et al. 2010). To
188 determine if this motif was also absent in the other two non-bilaterian taxa (Placozoa
189 and Ctenophora), the functional domains of Axin proteins in the four non-bilaterian
190 taxa and some selected bilaterian taxa were annotated using the webtool SMART
191 (Simple Modular Architecture Research Tool: http://smart.embl-heidelberg.de) and the

192 Axin proteins were aligned using Clustal Omega. This analysis showed that while the
193 βcatBM was identified in all bilaterian Axins, we could not identify this motif in Axin
194 proteins from the four non-bilaterian taxa (Supplementary Table 1). These observations
195 indicated that the βcatBM may have appeared in Axin after the divergence of the last
196 common ancestor of Bilateria and Cnidaria, or that the domain had diverged during
197 bilaterian evolution to render it undetectable in non-bilaterian Axin using the
198 bioinformatic tools we used. These observations also raised the possibility that in the
199 absence of a βcatBM non-bilaterian Axin would not be able to directly regulate β-catenin
200 stability in the cWnt DC.
201

202 ***NvAxin and NvAPC-like regulate cWnt signaling in Nematostella embryos***

203 We have previously shown that a bilaterian Axin protein can disrupt early
204 development in *Nematostella* (Kumburegama et al. 2011). But to the best of our
205 knowledge, a functional role for a non-bilaterian Axin in regulating cWnt signaling has
206 not been examined. To study Axin function in *Nematostella*, we first examined the
207 expression pattern of *NvAxin* in eggs and early embryos using whole mount in situ
208 hybridization (WMISH) (Supplementary Fig. 1). WMISH revealed that *NvAxin* was
209 expressed ubiquitously at the egg, cleavage and blastula stages (Supplementary Fig. 1A-
210 C). However, starting at the early gastrula stage, *NvAxin* displayed an asymmetrical
211 expression pattern with the mRNA mostly restricted to the future oral pole and this
212 expression persisted through the planula stage (Supplementary Fig. 1D-F). This
213 expression pattern suggested a function for the NvAxin protein in regulating early
214 pattern formation in *Nematostella*.

215 We next asked if disrupting *NvAxin* function affected cWnt signaling during early
216 *Nematostella* development. It is now well established that cWnt signaling regulates cell
217 fates along the animal-vegetal axis in *Nematostella* (Wikramanayake et al. 2003; Lee et
218 al. 2007; Röttinger et al. 2012; Lebedeva et al. 2021; Wijesena et al. 2022). Blocking β-
219 catenin signaling using a dominant-negative form of NvTcf that prevents β-catenin from
220 interacting with cis-regulatory elements of cWnt target genes leads to the disruption of
221 normal gastrulation and downregulation of genes in cell types derived from animal half
222 blastomeres—the endomesoderm and pharynx (Röttinger et al. 2012) (Supplementary
223 Fig. 2). To determine if NvAxin regulates cWnt signaling and the nuclearization of β-
224 catenin in embryos, we co-expressed NvAxin-GFP with Nvβ-catenin-mCherry by mRNA
225 injection into zygotes and examined developing embryos for Nvβ-catenin-mCherry
226 expression at the blastula stage. Our results showed that while control embryos co-
227 injected with *GFP* and *Nvβ-catenin-mCherry* mRNA exhibited nuclearization of Nvβ-
228 catenin-mCherry protein on one side of the embryo, embryos co-expressing either
229 NvAxin-GFP or Axin-GFP from the sea urchin *Strongylocentrotus purpuratus* (SpAxin-
230 GFP) and Nvβ-catenin-mCherry did not display any nuclear localization of Nvβ-catenin-
231 mCherry (Fig. 2A-C). This result indicated that NvAxin overexpression blocks
232 nuclearization of Nvβ-catenin-mCherry, presumably by mediating phosphorylation and
233 destabilization of β-catenin within the DC.

234 Earlier studies had demonstrated that overexpression of sea urchin Axin, NvDvl-
235 DIX (a dominant-negative form of Dvl for cWnt signaling), a repressive form of β-
236 catenin and dominant-negative NvTcf produced a similar phenotype in *Nematostella*
237 embryos where the overexpression of the proteins blocked cWnt signaling, but primary
238 archenteron invagination still occurred (Lee et al. 2007; Kumburegama et al. 2011;

239 Röttinger et al. 2012). These studies noted that while the embryos in which cWnt was
240 downregulated initially formed an endodermal epithelium, this epithelium appeared to
241 disintegrate by the late gastrula stage (Kumburegama et al. 2011; Röttinger et al. 2012).
242 Consistent with these previous observations, overexpression of NvAxin in embryos by
243 mRNA injection into zygotes produced embryos that underwent primary archenteron
244 invagination, and these embryos failed to maintain a normal gut epithelium compared
245 to embryos expressing GFP (Fig. 2D-F).

246 We next investigated if manipulating Axin levels in *Nematostella* embryos had an
247 effect on endogenous gene expression consistent with a function for the protein in the
248 cWnt DC. We reasoned that overexpressing NvAxin would lead to a downregulation of
249 cWnt-dependent gene expression while knockdown or knockout of NvAxin would lead
250 to an increased expression of these genes. Consistent with these predictions, assaying
251 NvAxin- or SpAxin-overexpressing *Nematostella* embryos for gene expression in syn-
252 expression domains (Röttinger et al. 2012) (see Fig. 2G) using qPCR showed a
253 downregulation of genes expressed in the central domain and central ring (see Fig. 2G)
254 and an upregulation of genes expressed in the apical domain compared to control
255 embryos (Fig 2H,I). Conversely, knockdown of NvAxin using antisense morpholinos led
256 to an upregulation of genes expressed in the central domain, central ring, and external
257 ring while genes expressed in the apical domain were downregulated (Supplementary
258 Fig. 3A). To compare the changes in gene expression following knockdown of NvAxin
259 with the changes in gene expression caused by knockdown of NvAPC-like, we injected
260 antisense morpholinos against NvAPC-like into zygotes and used qPCR to analyze gene
261 expression in these embryos. Consistent with the effect we noted in NvAxin knockdown

262 embryos, we saw an upregulation of genes expressed in the central domain and the
263 central ring in NvAPC-like MO injected embryos (Supplementary Fig. 3B).
264 To use an additional strategy to assess the effect of Axin downregulation on cWnt
265 signaling in *Nematostella* embryos we carried out a CRISPR/Cas9-mediated NvAxin
266 knockout experiment. To compare the molecular phenotypes between *NvAPC-like* and
267 *NvAxin* knockout embryos we also designed an *NvAPC-like* single guide RNA (gRNA) to
268 introduce a mutation into *NvAPC-like* in *Nematostella* embryos. The *NvAxin* and
269 *NvAPC* gRNAs and Cas9 enzyme were injected into zygotes and animals were observed
270 when control Cas9-only injected animals were at the four-tentacle polyp stage. We
271 noted that *Nematostella* polyps developing from zygotes injected with *Axin* gRNA/Cas9
272 and *APC-like* gRNA/Cas9 had supernumerary tentacles (Kraus et al. 2016) (Fig. 3Aa,
273 Ab, Ac). Animals injected with *Axin* plus *APC-like* gRNA with Cas9 typically showed a
274 more severe phenotype with additional ectopic tentacles present throughout the animal
275 (Fig. 3Ad). The NvAxin gRNA-mediated genome editing was validated by sequencing
276 around the NvAxin gRNA excise sites in four single NvAxin gRNA-injected embryos and
277 one Cas9-injected embryo (Supplementary Fig. 4) and by using WMISH to detect
278 *NvAxin* expression in CRISPR/Cas9-mediated knockout embryos compared with Cas9-
279 injected control embryos at 24 hpf (Fig. 3B). WMISH showed that 81.9% of the control
280 embryos showed strong *NvAxin* expression at the animal pole; 13.7% showed detectable
281 but weaker asymmetrical *NvAxin* expression, and 4.4% showed no detectable signal
282 (n=204) (Fig. 3Ba). By contrast, 72.5% of NvAxin gRNA/Cas9-injected embryos showed
283 no detectable *Axin* expression, 24.4% showed weak *Axin* expression, and only 3.1%
284 showed a signal like that seen in the control (n=131) (Fig. 3Bb). The embryos with weak
285 *NvAxin* signals may be due to incomplete excision of NvAxin or the generation of

286 mosaic embryos where the gene was only excised in some nuclei. The percentage of
287 successful excisions using CRISPR/Cas9 noted in this study are consistent with other
288 studies that have used CRISPR/Cas9 to carry out gene editing in *Nematostella* embryos
289 (Kraus et al. 2016; Servetnick et al. 2017).

290 To evaluate the effect of CRISPR/Cas9-mediated *Axin* and *APC-like* knockout on
291 cWnt-dependent gene expression during early embryonic development, we used qPCR
292 analysis and the results revealed that the genes expressed in the central domain and
293 central ring were all upregulated indicating that knockout of *NvAxin* and *NvAPC-like*
294 led to increased cWnt signaling consistent with a function for NvAxin and NvAPC-like in
295 the cWnt DC (Fig. 3C,D). The qPCR analysis also revealed that the apical domain genes
296 *Fz5* and *Six3* were downregulated, consistent with previous studies showing that global
297 upregulation of cWnt signaling leads to the downregulation of genes expressed in the
298 apical domain (Röttinger et al. 2012) (Fig. 3C,D). Notably, *NvWnt8* and *Nvlhx6* (a gene
299 expressed in the external ring) exhibited a stronger upregulation in both *NvAxin* gRNA
300 and *NvAPC-like* gRNA-injected embryos than other genes expressed at the animal pole,
301 suggesting that these genes are particularly sensitive to levels of cWnt signaling. Hence,
302 disruption of either one of the two core scaffold proteins in the *Nematostella* DC likely
303 resulted in the strong activation of *Wnt8* and *lhx6* expression. Alternatively, *NvWnt8*
304 and *Nvlhx6* might be repressed by cWnt outside their normal domain of expression and
305 are ectopically expressed when cWnt is downregulated. In sum, these results provided
306 strong evidence that Axin plays a crucial role in negatively regulating cWnt signaling in
307 *Nematostella* embryos and indicated that NvAxin has a role in the cWnt DC even
308 though it lacks a distinct β-catenin binding motif. Additionally, these experiments
309 showed that NvAPC-like regulates cWnt signaling even though it lacks most of the

310 domains shown be required for APC function in the DC in bilaterians. Our work also
311 corroborated the work of Kraus et al. (2016) who previously showed that NvAPC-like
312 regulates cWnt signaling in *Nematostella*.
313

314 ***Nematostella Axin overexpression disrupts cWnt signaling in sea urchin***
315 ***embryos***

316 We next sought to determine if *Nematostella* Axin could regulate cWnt signaling
317 in a bilaterian. Extensive work done in sea urchin embryos has shown that the cWnt
318 pathway plays a critical role in specifying and patterning the anterior-posterior (AP)
319 axis, and blocking β-catenin nuclearization in early embryos produces a unique
320 anteriorized phenotype hence making these embryos useful for assaying cWnt signaling
321 (Wikramanayake et al. 1998; Logan et al. 1999; Sun et al. 2021). When we expressed sea
322 urchin β-catenin-mCherry (Spβ-catenin-mCherry) in sea urchin embryos by mRNA
323 injection into zygotes, live imaging showed typical nuclearization of Spβ-catenin-
324 mCherry at the vegetal pole (Wikramanayake et al. 1998; Logan et al. 1999; Sun et al.
325 2021) (Fig. 4Aa). However, when Spβ-catenin-mCherry was co-expressed with NvAxin
326 or SpAxin in sea urchin embryos there was complete elimination of Spβ-catenin-
327 mCherry nuclearization (Fig. 4Ab, Ac). Moreover, consistent with previous observations
328 in sea urchin embryos where blocking Spβ-catenin nuclearization by SpAxin
329 overexpression led to severe anteriorization of sea urchin embryos (Sun et al. 2021) (Fig.
330 4Ba,Bb), overexpression of NvAxin in sea urchin embryos also led to a phenotype
331 indistinguishable from the phenotype generated from SpAxin overexpression (Fig. 4Bc).
332 Importantly, the anteriorized embryos were not able to recover even when control
333 animals were at the pluteus larval stage (Fig. 4Ba'-c') (Wikramanayake et al. 1998; Sun

334 et al. 2021). Consistent with the anteriorized phenotype, analysis of gene expression in
335 sea urchin embryos overexpressing NvAxin and SpAxin showed that all seven
336 endomesoderm gene markers tested were significantly downregulated, while two
337 neuroectoderm gene markers were upregulated (Fig. 4C, D). These experiments
338 demonstrated that NvAxin is a strong regulator of cWnt signaling in a bilaterian, even
339 though it lacks the conserved βcatBM.
340

341 ***The NvAxin GSK-3β binding domain is required for its function in the***
342 ***cWnt pathway***

343 In bilaterians, the βcatBM on Axin is critical for the protein to interact with and
344 target β-catenin for degradation during activation of cWnt signaling (Ikeda et al. 1998;
345 Xing et al. 2003; Stamos and Weis 2013). Bioinformatic analysis using SMART
346 indicated that NvAxin lacks the βcatBM but it has the APC- (RGS), GSK- (GID), and
347 Dvl- (DAX) binding domains, which are also found in the Axin proteins of other non-
348 bilaterians (Supplementary Table 1). Since our studies showed that NvAxin could
349 regulate β-catenin nuclearization in the sea urchin embryo, we used a rescue assay that
350 we had previously developed in sea urchins (Sun et al. 2021) to identify the domains on
351 NvAxin required for β-catenin regulation in the cWnt pathway. This rescue assay takes
352 advantage of the unique "posteriorized" phenotype produced in sea urchin embryos
353 when levels of Axin in the embryo are reduced using an anti-sea urchin Axin
354 morpholino, which can be rescued by overexpressing the wildtype Axin protein (Sun et
355 al. 2021) (Fig. 5A-C). We showed that while injection of a control MO has no effect on
356 embryo development, injections of an anti-sea urchin (*Lytechinus variegatus*, Lv) Axin
357 MO produces a posteriorized phenotype, and additionally, while *GFP* RNA control

358

359

360 injections have no effect on development, *NvAxin* RNA injection anteriorizes sea urchin
361 embryos (Fig. 5Ba-d'). To determine if NvAxin could rescue sea urchin embryos
362 posteriorized by injection of the LvAxin MO, we co-injected the LvAxin MO with full-
363 length *NvAxin* mRNA. Examination of these embryos showed that while the embryos
364 co-injected with the LvAxin MO and *GFP* mRNA were posteriorized as expected (Fig.
365 5Ca,a'), the embryos co-injected with the LvAxin MO and *NvAxin* mRNA were
366 completely rescued (Fig. 5Cb,b'). Similarly, co-injection of the LvAxin morpholino with
367 *NvAxinΔRGS* mRNA or *NvAxinΔDAX* mRNA efficiently rescued the posteriorized
368 phenotype induced by the LvAxin morpholino in sea urchins (Fig. 5Cc-d'). However, co-
369 injection of the LvAxin MO with *NvAxinΔGID* mRNA failed to rescue the phenotype
370 (Fig. 5Ce,e') indicating the requirement of the GSK-3β binding domain (GID) for
371 NvAxin to function in the cWnt DC. This result is consistent with our observations in
372 sea urchin embryos, where the SpAxinΔGID construct was also unable to rescue Axin
373 knockdown embryos (Sun et al. 2021). We conclude that the GID domain is likely the
374 most crucial domain of NvAxin for regulating β-catenin stability in the cWnt DC.
375 Previous studies in bilaterians have shown that overexpression of the Axin GID
376 peptide alone is sufficient to activate cWnt signaling (Hedgepeth et al. 1999; Sun et al.
377 2021). The underlying mechanism for this is still unclear but it has been suggested that
378 the GID domain can bind to endogenous GSK-3β and prevent it from interacting with
379 Axin (Hedgepeth et al. 1999; Chou et al. 2006; Sun et al. 2021). Our NvAxin rescue
380 experiments in sea urchins using Axin domain-deletion constructs clearly showed that
381 the GID domain is required for NvAxin's activity in the cWnt destruction complex (Fig.

382 5Ce,e'). GSK-3β binding to Axin is a critical step in assembling the DC in bilaterians. To
383 begin to assess if the NvAxin-GID (NvGID) domain was involved in regulating GSK-3β
384 in *Nematostella* we first overexpressed an NvGID-GFP construct in embryos by
385 microinjection of mRNA into zygotes. When control animals were at the polyp stage,
386 the NvGID-GFP overexpressing embryos had a morphology resembling *Nematostella*
387 embryos overexpressing an activated form of β-catenin (Röttinger et al. 2012) (Fig. 6A).
388 Analysis of germ layer-specific markers at the blastula stage using qPCR showed that
389 endomesoderm gene markers and pharyngeal markers were highly upregulated while
390 the ectoderm gene markers were downregulated (Fig. 6B). These results are consistent
391 with the notion that as seen in bilaterians, Axin-GID overexpression can activate cWnt
392 signaling and provides additional evidence that NvAxin scaffolds a critical DC
393 component similar to bilaterian Axin.

394 The residues within the GID domain mediating interaction between Axin and
395 GSK-3β are highly conserved in bilaterians and all four non-bilaterian taxa (Kremer et
396 al. 2010) (Supplementary Fig. 5). The conservation of the NvGID suggested that the
397 phenotype elicited by overexpression of the peptide in *Nematostella* was due to it
398 directly binding to NvGSK-3β and preventing NvGSK-3β from binding to NvAxin. To
399 validate this predicted interaction, we mixed NvGID-GFP and NvGSK-3β-mCherry
400 proteins made using *in vitro* transcription and translation (TnT) and
401 immunoprecipitated (IP) NvGID-GFP using anti-GFP antibodies. Western blot analysis
402 of the IP samples using anti-mCherry antibodies showed a clear interaction between
403 NvGID-GFP and NvGSK-3β-mCherry *in vitro* (Fig. 6C). These results demonstrated
404 that NvGID directly interacts with NvGSK-3β and further supports the notion that
405 NvAxin has an activity consistent with it being part of a DC in *Nematostella*.

406 It is important to note that the morphological and molecular phenotypes
407 generated from upregulating cWnt signaling by overexpression of NvGID, and NvAxin
408 and NvAPC-like knock down/knock out using morpholinos and CRISPR/Cas-9 show
409 some significant differences (compare Fig. 3 with Fig. 6). When NvAxin-GID was
410 overexpressed in *Nematostella* embryos, the embryos did not form a polyp stage like
411 controls, but rather had what appeared to be a hollow and expanded swollen appearance
412 (Fig. 6A). Gene expression analysis showed that these embryos had elevated expression
413 of genes expressed in the central domain, central ring and external ring and reduction in
414 expression of genes expressed in the apical domain. These embryos resemble the
415 phenotypes generated when ectopically activating cWnt signaling by overexpressing a
416 constitutively activate form of β-catenin (Röttinger et al. 2012). Both these methods are
417 likely to activate early cWnt signaling thus impacting early cell fate specification in
418 *Nematostella* embryos. It is likely that there is Axin and APC-like mRNA and protein in
419 the egg and early embryo and hence, when using morpholinos and CRISPR/Cas-9 to
420 knock down or knock out Axin and APC-like, these methods do not impact the
421 maternally loaded molecules. We suggest that the Axin and APC-like knock-
422 down/knock-out phenotypes are due to elevated cWnt signaling affecting oral-aboral
423 axis patterning, a relatively late event, and not early cell fate specification.
424

425 ***In vitro and in vivo protein-protein interaction assays indicate that the***
426 ***Nematostella Destruction Complex proteins have binding activities***
427 ***previously undefined in bilaterians***

428 Previous studies in bilaterian taxa such as vertebrates and dipterans have shown
429 interactions between Axin-APC, Axin-β-catenin, APC-β-catenin, APC-GSK-3β and Axin-

430 GSK-3β *in vitro* and *in vivo* and in general, the protein binding interfaces for these
431 interactions have been well defined (Ikeda et al. 1998; Kishida et al. 1998; Dajani et al.
432 2003; Ha et al. 2004; Peterson-Nedry et al. 2008; Kremer et al. 2010; Roberts et al.
433 2011; Pronobis et al. 2015; Ranes et al. 2021). These studies have also demonstrated
434 that while there is a single defined β-catenin binding domain on bilaterian Axin, there
435 are multiple β-catenin binding domains on APC that have distinct sequence motifs
436 (Roberts et al. 2011; Pronobis et al. 2015; van Kappel and Maurice 2017; Pronobis et al.
437 2017). The experimental analyses that we have done in this study showed that both
438 NvAxin and NvAPC-like regulate cWnt in *Nematostella*. Hence, the lack of critical
439 domains required for cWnt DC activity in NvAxin and NvAPC-like prompted us to
440 investigate if these proteins could still form a functional DC perhaps through protein
441 binding domains previously uncharacterized in bilaterians. To explore this possibility,
442 we synthesized GFP-tagged NvAxin and SpAxin, and mCherry-tagged Nvβ-catenin, Spβ-
443 catenin, NvGSK-3β and SpGSK-3β using *in vitro* TnT and then mixed the various
444 protein pairs and used an anti-GFP antibody to IP the GFP tagged Axin proteins. We
445 then probed Western blots of the immunoprecipitated proteins with anti-mCherry
446 antibodies to evaluate any interaction between the protein pairs. As expected, this assay
447 revealed a robust interaction between sea urchin Axin-GFP and sea urchin β-catenin-
448 mCherry (Fig. 7A, Lane 5). We also noted a weaker but persistent interaction between
449 NvAxin and Nvβ-catenin and NvAxin and Spβ-catenin proteins in vitro (Fig. 7A, Lane
450 1,2). This was unexpected since NvAxin does not have the well-defined βcatBM seen in
451 bilaterian Axin (Fig. 1C).

452 We next asked if sea urchin Axin (which has the conserved βcatBM) could
453 interact with Nvβ-catenin. To our surprise, despite sea urchin Axin containing a

454 conserved βcatBM and a demonstrated ability to strongly interact with sea urchin β-
455 catenin *in vitro*, it only displayed a weaker interaction with Nvβ-catenin in this assay
456 (Compare Fig. 7A, Lane 4 and Lane 5). These results suggested that the Axin interacting
457 domains on Nvβ-catenin (the armadillo repeats) had diverged from the corresponding
458 domains on bilaterian β-catenin, and hence it was unable to interact strongly with a
459 bilaterian Axin. *Nematostella* β-catenin has all 12 ARM domains seen in bilaterians and
460 each of its ARM repeats has a high level of homology to corresponding ARM domains in
461 bilaterian β-catenin indicating a strong conservation over 700 million years of evolution
462 (Schneider et al. 2003). Hence, any changes in Nvβ-catenin protein that affects how it
463 interacts with a bilaterian Axin βcatBM would likely be more subtle amino acid changes
464 that affects binding affinity between the proteins. In sum, these experiments showed
465 that NvAxin can directly interact with *Nematostella* and sea urchin β-catenin, but based
466 on the *in vitro* assay, these interactions appeared considerably weaker than the
467 interaction between sea urchin Axin and sea urchin β-catenin.

468 We then investigated if NvAxin could directly interact with NvGSK-3β using the
469 *in vitro* pull-down assay. As predicted by the presence of a conserved GID on NvAxin
470 and our previous observation that the NvGID could interact with NvGSK-3β, Western
471 blotting of the IP products showed a clear interaction between NvAxin-GFP and NvGSK-
472 3β-mCherry (Fig. 7A, Lane 3). Likewise, our results showed that sea urchin Axin-GFP
473 interacted strongly with sea urchin GSK-3β-mCherry (Fig. 7A, Lane 6). It is notable that
474 the Axin GID domain is highly conserved, including in ctenophores (Supplementary Fig.
475 5), indicating that the Axin-GSK-3β interaction evolved over 700 mya.

476 In bilaterians, Axin and APC proteins heterodimerize to form the scaffold for the
477 β-catenin DC. Bilaterian APC/APC-like proteins have a complex domain structure that

478 allows them to interact with several proteins including Axin and β-catenin. NvAPC-like
479 is smaller in size than the vertebrate or dipteran proteins, and it lacks many of the
480 domains shown to bind to β-catenin and Axin in bilaterians (Fig. 1D; Roberts et al. 2011;
481 Pronobis et al. 2015; Pronobis et al. 2017; Ranes et al. 2021). When we analyzed
482 NvAPC-like domain structure using the webtool SMART (Simple Modular Architecture
483 Research Tool), we noted that it had seven conserved armadillo repeats and two poorly
484 characterized repeat regions at the N-terminus. NvAPC-like also lacked the SAMP
485 domains that are critical for bilaterian Axin-APC interaction (Pronobis et al. 2015;
486 Pronobis et al. 2017) (Fig. 1D). To determine if NvAPC-like (tagged with mCherry)
487 could directly interact with NvAxin, Nvβ-catenin and NvGSK (tagged with GFP), we
488 carried out the *in vitro* protein-protein interaction assay previously described. We
489 noted that NvAPC-like-mCherry robustly interacted with Nvβ-catenin-GFP in this assay
490 (Fig. 7B). We were also able to detect interactions between NvAPC-like-mCherry and
491 NvGSK-3β-GFP and NvAPC-like-mCherry and NvAxin-GFP *in vitro* (Fig. 7B).
492 The *in vitro* assay that we used in the experiments described above provides
493 insight into potential direct interactions between components of the cWnt DC in
494 *Nematostella* embryos. However, in those cases where we saw weak interactions *in*
495 *vitro*, it is possible that in the *in vivo* environment, post-translational modifications or
496 bridging by other proteins in the embryo lead to higher affinity interactions (Ha et al.
497 2004; Kimelman and Xu 2006; Pronobis et al. 2015; Ranes et al. 2021). To validate the
498 results that we saw in the *in vitro* experiments with an *in vivo* and *ex vivo* approach, we
499 adopted the split Click Beetle Green (CBG) luciferase system (Villalobos et al. 2010)
500 (Supplementary Fig. 6). Axin and β-catenin proteins from *Nematostella* and the sea
501 urchin *S. purpuratus* were tagged with split CBG luciferase (Villalobos et al. 2010). All

502 possible pairs of split-luciferase-tagged Axin and β-catenin proteins from the same or
503 different species, were expressed in *Nematostella* embryos by mRNA injection into
504 zygotes. The luminescence of split luciferase was measured in live embryos or in
505 embryo lysates. Normalized kinetic curves from embryonic lysates and live embryos are
506 shown in Supplemental Fig. 6. Consistent with the *in vitro* studies, SpAxin + Spβ-
507 catenin had the highest signal in both embryonic lysates and live embryos, while NvAxin
508 + Spβ-catenin had clear but relatively lower signal (Supplemental Fig. 6A, B). However,
509 SpAxin did not appear to interact with Nvβ-catenin in either embryonic lysates or live
510 embryos (11 % and 10 % of SpAxin + Nvβ-catenin signal, respectively). This result is
511 inconsistent with the *in vitro* pull-down experiments where we noted a weak interaction
512 between SpAxin and Nvβ-catenin (Fig. 7, Lane 4). The reason for this discrepancy is not
513 known at this time. Interestingly, NvAxin + Nvβ-catenin yielded a relatively low signal
514 (27% of NvAxin + Nvβ-catenin intensity) in live embryos but virtually none in lysates
515 (13 %). These observations suggest that this interaction requires the presence of intact
516 cellular and molecular complexes that are lost in lysates. However, overall, the
517 interactions between NvAxin + Nvβ-catenin, NvAxin + Spβ-catenin, and SpAxin + Spβ-
518 catenin were consistent between the *in vitro* and *in vivo* approaches and gives credence
519 to the notion that the interaction between NvAxin and Nvβ-catenin is weaker than the
520 interaction between SpAxin and Spβ-catenin. Moreover, the *in vivo* and *ex vivo*
521 experiments confirmed that NvAxin and Nvβ-catenin, and SpAxin and Nvβ-catenin are
522 only capable of relatively weak interactions most likely discounting a major *in vivo* role
523 for bridging proteins or post-translational modifications to enhance these interactions.
524

525 ***AlphaFold software predicts novel protein-binding interfaces between***
526 ***cWnt Destruction Complex components in Nematostella***

527 The unexpected direct protein-protein interactions we noted in the *in vitro* assays
528 prompted us to use AlphaFold3 to determine if the AI-based program would be able to
529 predict the binding interfaces between the respective protein pairs. As expected,
530 AlphaFold analysis predicted the interactions between SpAxin-Spβ-catenin and
531 SpAxin-SpGSK-3β based on complementary domains seen in orthologs from other
532 bilaterian proteins (Supplementary Fig. 7A, B). Moreover, as expected from the
533 conserved domains, AlphaFold also predicted an interaction between NvAxin and
534 NvGSK-3β (Supplementary Fig. 7C). The AlphaFold analysis also indicated possible
535 interactions between NvAxin-Nvβ-catenin and NvAPC-like-Nvβ-catenin based on the
536 iPTM and PTM values (Supplementary Fig. 7D, E). This was unexpected because
537 NvAxin and NvAPC-like lack the β-catenin-interaction domains extensively
538 characterized in bilaterians (Roberts et al. 2011; Pronobis et al. 2015; Pronobis et al.
539 2017; Ranes et al. 2021). In contrast, even though the *in vitro* assays showed
540 interactions between NvAxin-NvAPC-like and NvAPC-like-NvGSK-3β, these
541 interactions were not supported by AlphaFold analysis. (Supplementary Fig. 7F, G).
542 This may be due to the NvAPC-like being a relatively large protein and in some such
543 cases AlphaFold is not as efficient in predicting protein-protein interactions (Bryant et
544 al. 2022; Shor and Schneidman-Duhovny 2024).

545 When we used AlphaFold3 and ChimeraX (Meng et al. 2023) to analyze
546 predicted and visualized interactions sites between the NvAPC-like and Nvβ-catenin,
547 we identified an α-helix interaction site within the ARM 708-753aa region (first ARM

548 domain) of NvAPC-like. This region was predicted to interact with Nvβ-catenin with
549 high iPTM and PTM values (Supplementary Fig. 7H). Notably, this ARM sequence is
550 conserved across *H. sapiens*, *D. melanogaster*, *S. purpuratus* and *N. vectensis* (amino
551 acid identity > 41%). We did not analyze the potential interactions of the other six
552 NvAPC-like ARM domains with Nvβ-catenin. Finally, we analyzed NvAPC-like protein
553 structure for a potential interaction with the NvAxin-RGS domain and AlphaFold
554 strongly predicted an interaction between the NvAxin-RGS and Repeat 1 of NvAPC-like
555 (Supplementary Fig. 7I) but not Repeat 2 (not shown).

556 The persistent, albeit weak, *in vitro* and *in vivo* interactions we noted between
557 NvAxin and Nvβ-catenin (Fig. 7, Supplementary Fig. 6) and the prediction of an
558 interaction between these proteins by AlphaFold3 analysis (Supplementary Fig. 7D)
559 were unexpected. AlphaFold 3 and ChimeraX software predicted two possible regions of
560 interaction between NvAxin and Nvβ-catenin, one located within the NvAxin-RGS
561 domain, and the other closer to the C-terminus of NvAxin (Figure 7C; Supplementary
562 Fig. 8A,B). Alignment of the predicted NvAxin-Nvβ-catenin interaction site on NvAxin
563 with the highly conserved βcatBM in bilaterian Axins using Clustal Omega and Jalview
564 showed some highly conserved amino acids between these sequences (Supplementary
565 Fig. 8F). The amino acid identity between the sequence in NvAxin-RGS and the second
566 sequence closer to the C-terminus, and the bilaterian βcatBM ranged from 20-26% and
567 11-28% respectively and we designated these sequences as "βcatBM-like". Significantly,
568 the leucines at positions 119 and 434 in the βcatBM-like sequences corresponds to a
569 leucine residue known to be essential for the interaction between bilaterian Axin and β-
570 catenin (Kremer et al. 2010) (Supplementary Fig. 8F). Additionally, Kremer et al.

571 (2010) identified a histidine residue at position 504 in *Drosophila* Axin as being critical
572 for β-catenin interaction with Axin. In *Nematostella* Axin, this corresponding residue is
573 missing, possibly accounting for the weak interaction between NvAxin and Nvβ-catenin.
574 We then examined Axin sequences from several other cnidarians to ask if similar
575 duplicated βcatBM-like sequences were present in the Axin proteins. Interestingly, the
576 predicted Axin-β-catenin binding sites are all located within the RGS domain
577 (Supplementary Fig. 9A) and C-terminal (Supplementary Fig. 9B) of Axin and are highly
578 conserved in each of these taxa. We also carried out AlphaFold and ChimeraX analysis
579 of predicted interactions between Axin and β-catenin in *Tricoplax adhaerens* (a
580 placozoan), *A. queenslandica* (a poriferan) and *Mnemiopsis leidyi* (a ctenophore). This
581 analysis predicted a single putative interaction site between Axin and β-catenin in these
582 species (Supplementary Fig. 8C,D,E,F). Alignment between the identified βcatBM-like
583 sequence on the ctenophore MlAxin-RGS and the bilaterian βcatBM did not reveal
584 conservation of the leucine residue; instead, an aspartic acid was identified
585 (Supplementary Fig. 8F). However, the identified βcatBM-like sequences on AqAxin-
586 RGS and TaAxin-RGS retained the conserved leucine associated with functional binding
587 (Kremer et al. 2010) (Supplementary Fig. 8F). The amino acid identities between the
588 βcatBM-like sequences in the RGS domain of TaAxin, AqAxin and MlAxin, and the
589 bilaterian βcatBM ranged from 16-33%, 12-25% and 21-28% respectively. We used
590 AlphaFold software to determine if the RGS domains of bilaterian Axins, including all
591 the bilaterian species listed in Supplementary Table 1, contained any putative β-catenin
592 interaction motifs, but we were not able to detect any such sequences (not shown).
593 Ctenophores are now widely believed to be the earliest-emerging metazoan group
594 (Dunn et al. 2008; Schultz et al. 2023). Consistent with this notion, the βcatBM-like

595 sequence on MlAxin identified using AlphaFold3 and ChimeraX lacked the conserved
596 leucine residue that is present in Axins from the other three non-bilaterian taxa. This
597 leucine along with a conserved histidine have been implicated as the two critical amino
598 acids involved in Axin-β-catenin interaction in bilaterians. The absence of both the
599 leucine and the histidine from the βcatBM-like sequence in ctenophore Axin indicated
600 that it would not be able to directly interact with ctenophore β-catenin. Consistent with
601 this idea MlAxin and Mlβ-catenin did not show any direct interactions when tested
602 using the *in vitro* TnT assay (Supplementary Fig. 8G). We next addressed if the
603 conserved leucine residues seen in the two βcatBM-like sequences in NvAxin were
604 responsible for the "weak" binding of NvAxin and Nvβ-catenin. We used site-directed
605 mutagenesis to change the conserved leucine in each of the βcatBM-like sequences in
606 NvAxin to aspartic acid to resemble the ctenophore βcatBM-like sequence and tested the
607 ability of these mutant NvAxin proteins to interact with Nvβ-catenin. Our analysis
608 showed that mutating the conserved leucine on each of the two βcatBM-like sequences
609 on NvAxin to aspartic acid reduced interaction with Nvβ-catenin compared to the wild-
610 type NvAxin βcatBM-like sequence, and mutating both leucines to aspartic acid
611 completely abolished interactions between NvAxin and Nvβ-catenin (Fig. 8C). In sum,
612 these results suggest that the bilaterian βcatBM evolved as a sequence on the Axin-RGS
613 with poor ability to interact with β-catenin and during pre-bilaterian evolution this
614 sequence acquired a critical leucine sequence that permitted weak interactions with β-
615 catenin.
616
617 **Discussion**

618 Studies on the evolution of metazoan signaling transduction pathways have been
619 impeded by the limited understanding of their roles in early emerging taxa and the
620 challenges to doing functional studies in these animals. We took advantage of the ability
621 to experimentally manipulate cWnt signaling in *Nematostella* embryos and the *in vitro*
622 assays we developed to identify direct protein interactions, coupled with the use of AI
623 tools to study the evolution of the cWnt destruction complex. We show that
624 *Nematostella* Axin and APC—which lack many of the domains required for bilaterian
625 DC function—can effectively regulate the stability of cytoplasmic β-catenin using
626 protein-protein interaction interfaces that to the best of our knowledge were previously
627 undefined in bilaterians. We also traced the evolution of the critical bilaterian Axin β-
628 catBM and provide evidence that it first appeared as a short β-catBM-like sequence
629 embedded in the Axin-RGS domain in the earliest branching metazoans. Our analysis
630 further indicates that during pre-bilaterian evolution the Axin β-catBM gained a leucine
631 residue that permitted weak direct interactions between Axin and β-catenin. The β-
632 catBM evolved in bilaterians through duplication of the β-catBM-like sequence in the
633 cnidarian-bilaterian last common ancestor (LCA) with the duplicated sequence inserted
634 towards the C-terminus of Axin. Our observations also suggest that in the Bilaterian
635 lineage the duplicated β-catBM-like sequence gained a higher affinity for β-catenin
636 through acquisition of additional amino acids, including a highly conserved histidine,
637 and the original β-catBM-like sequence was lost, most likely through drift. Overall, this
638 work has provided novel insight into the functional evolution of a major metazoan signal
639 transduction pathway.
640

641 **NvAxin and NvAPC-like can assemble a functional destruction complex**
642 **using novel protein binding interfaces**

643 Axin and APC-like in cnidarians and other non-bilaterians lack the domains
644 defined in bilaterians for assembling a functional cWnt DC. Hence, to investigate if the
645 *Nematostella* DC could regulate cWnt signaling we carried out a series of experiments
646 using readouts for cWnt signaling that we have previously established (Wikramanayake
647 et al. 2003; Lee et al. 2007; Kumburegama et al. 2011; Röttinger et al. 2012; Sun et al.
648 2021). Our results showed that both NvAxin and NvAPC play a role in cWnt signaling,
649 and moreover, we showed that NvAxin can also regulate cWnt signaling in sea urchin
650 embryos (Fig. 4). We also used an *in vitro* protein-protein interaction assay to
651 determine if NvAxin and NvAPC are able to directly interact with each other and with
652 NvGSK-3β and Nvβ-catenin. This assay permitted us to identify previously undefined
653 interactions between DC components. For example, our *in vitro* experiments showed
654 that as predicted from NvAxin structure, this protein binds robustly to NvGSK-3β. This
655 assay also allowed us to detect weak interactions between NvAxin and Nvβ-catenin that
656 were unexpected because we were not able to identify a primary sequence that
657 resembled the bilaterian β-catBM on NvAxin using SMART software. But using AI tools
658 we were able to identify two β-catBM-like sequences on NvAxin. The *in vitro* assay also
659 allowed us to show that NvAPC-like binds robustly to Nvβ-catenin and this interaction
660 was also unexpected since NvAPC-like lacks the multiple domains that have been shown
661 to bind β-catenin in bilaterians (Adamska et al. 2010; Roberts et al. 2011; Nelson and
662 Näthke 2013; Pronobis et al. 2017; Abbott and Näthke 2023) (Fig. 1). Moreover, our *in*
663 *vitro* experiments showed that NvAxin and NvAPC-like can interact directly even in the
664 absence of the SAMP domains in NvAPC-like. Previous studies in *Drosophila* have

665 shown that DmAPC2 can interact with Axin in the absence of the SAMP domains
666 suggesting that some bilaterian APC proteins may also contain protein interaction
667 interfaces that have not been precisely defined previously (Roberts et al. 2011). We
668 suggest that in *Nematostella*, the interaction between NvAxin and NvAPC-like *in vivo*
669 would likely bring β-catenin and GSK-3β together for phosphorylation of the β-catenin
670 degron targeting the protein for degradation.

671 Other structural features of NvAPC-like indicated additional differences between
672 the *Nematostella* and bilaterian cWnt DCs in the molecular mechanisms targeting β-
673 catenin to the proteasome. Previous work has shown a clear role for NvAPC-like in
674 regulating cWnt signaling in *Nematostella* (Kraus et al. 2016) and our results
675 corroborated that work. However, the structure of NvAPC-like predicts that this protein
676 would be unable to target β-catenin to the proteasome. For example, APC proteins from
677 *Drosophila* and vertebrates have several 15 and 20 amino acid repeats that can bind to
678 β-catenin and in addition, these proteins have 2-3 SAMP domains that are involved in
679 dimerizing with Axin (Polakis 1995; Yang et al. 2006; Roberts et al. 2011; Nelson and
680 Näthke 2013; Pronobis et al. 2015; Abbott and Näthke 2023) (Fig. 1D). The second 20aa
681 repeat and an adjacent sequence are particularly significant because current models
682 propose that these domains are critical for transferring phosphorylated β-catenin from
683 Axin to APC prior to being moved to the proteasome for degradation (Kimelman and Xu
684 2006; Roberts et al. 2011; Pronobis et al. 2015). Strikingly, the NvAPC-like protein lacks
685 any detectable 15aa and 20aa repeats or the SAMP domains but has seven predicted
686 ARM repeats and two poorly characterized repeat regions (Fig. 1D). Hence, it appears
687 that NvAPC-like resembles a severely truncated bilaterian APC protein that would likely
688 be oncogenic in humans, and one that would not be predicted to regulate β-catenin

689 degradation (Polakis 1995; Kinzler and Vogelstein 1996; Fodde et al. 2001; Schneikert
690 and Behrens 2007). Despite these apparent structural deficits in cnidarian DC
691 scaffolding proteins experimental data in a number of cnidarian species has shown that
692 they can tightly regulate β-catenin protein stability in embryos. For example, when a β-
693 catenin-GFP fusion protein is expressed by mRNA injection in *Nematostella* and other
694 cnidarian embryos the protein is initially broadly expressed, but it is then cleared from
695 the vegetal pole blastomeres of the embryos and very tightly restricted to nuclei of the
696 animal pole blastomeres (Wikramanayake et al. 2003; Lee et al. 2007; Momose and
697 Houliston 2007; Momose et al. 2008; Kumburegama et al. 2011; Röttinger et al. 2012).
698 Hence, our observations raise important questions as to whether NvAPC-like has a role
699 in shuttling phosphorylated β-catenin to the proteasome, or if cnidarians have a
700 different mechanism to carry out this critical function. These are important questions
701 that need to addressed in future studies.

702 Another striking observation from our phylogenetic analysis of the Axin and
703 APC-like/APC proteins is the differential acquisition of domains between these proteins
704 during evolution. While we have not studied Axin domain evolution beyond the four
705 main domains (RGS, GID, βcatBM and DAX), Axin does not seem to have gained
706 additional domains other than the βcatBM with a high-affinity for β-catenin. In
707 contrast, the APC-like/APC proteins seem to have acquired many additional domains in
708 the bilaterian lineage likely through gene fusion (see Fig. 1) (Adamska et al. 2010;
709 Nelson and Näthke 2013; Abbott and Näthke 2023). This is particularly striking since
710 Axin and APC-like/APC most likely co-evolved in the cWnt DC and it would be a
711 reasonable prediction that changes in one protein would likely lead to changes in its
712 partner protein. Some of the additional domains acquired by bilaterian APC are likely

713 domains that are required for other functions of APC through its interactions with over
714 100 other previously identified proteins (Nelson and Näthke 2013). It is possible that
715 modeling the co-evolution of Axin and APC-like/APC may lead to some insights into the
716 evolutionary forces constraining the size of Axin while allowing the dramatic increase in
717 domain complexity and size in bilaterian APC-like/APC.
718

719 **Reconstructing the evolution of the bilaterian Axin β-catenin binding motif**

720 Our experimental work combined with the use of AI-enabled AlphaFold software
721 allowed us to propose a plausible mechanism for the evolution of the bilaterian Axin
722 βcatBM from pre-bilaterian antecedents. Insights into how the Axin βcatBM evolved
723 came from AlphaFold's identification of the NvAxin sequences underlying the weak but
724 consistent interactions we noticed between NvAxin and Nvβ-catenin *in vitro* and *in*
725 *vivo*. AlphaFold software predicted that two βcatBM-like sequences on NvAxin with
726 similarity to the conserved bilaterian βcatBM could potentially interact weakly with
727 Nvβ-catenin. But surprisingly one sequence was embedded within the NvAxin-RGS
728 domain and the other was closer to the C-terminus of Axin where the βcatBM is found in
729 bilaterian Axin (Fig. 8; Supplementary Fig. 8). Using AlphaFold we found a βcatBM-
730 like sequence embedded in the Axin-RGS domains in a placozoan, a sponge and three
731 ctenophores but we could not identify a second similar sequence closer to the C-
732 terminus in these taxa as we did in Axin from *Nematostella* and several other cnidarians
733 (Fig. 8; Supplementary Fig. 8,9). In addition, we could not identify a βcatBM-like
734 sequence in any bilaterian Axin-RGS. Within the two βcatBM-like sequences in NvAxin
735 and the single βcatBM-like sequence in TaAxin-RGS and AqAxin-RGS, there is a
736 conserved leucine residue, also seen in the bilaterian Axin βcatBM, that has been shown

737 to be critical for interaction between Axin and β-catenin in *Drosophila* (Kremer et al.
738 2010) (Fig. 8; Supplementary Fig. 8C,D,F). But the βcatBM-like sequences of NvAxin,
739 TaAxin and AqAxin lack a highly conserved histidine that has been shown to be critical
740 for Axin-β-catenin interactions in *Drosophila* (Kremer et al. 2010) (Supplementary Fig.
741 8C,D,F). Our analysis showed that the βcatBM-like sequence in the *Mnemiopsis* Axin-
742 RGS lacked both the conserved leucine and histidine residues required for interaction of
743 the *Drosophila* βcatBM with β-catenin and we showed that MlAxin and Mlβ-catenin
744 could not directly interact *in vitro* (Supplementary Fig. 8E,F).

745 It is now established that ctenophores are likely the earliest emerging metazoan
746 taxon (Dunn et al. 2008; Schultz et al. 2023). Hence, based on metazoan phylogeny we
747 can infer that the putative ancestral βcatBM-like sequence that was present in the Axin-
748 RGS domain in the "urmetazoan" acquired a leucine residue in the βcatBM-like
749 sequence prior to the split of the poriferans from a last common ancestor (LCA) to
750 placozoans, cnidarians and bilaterians. An alternative scenario is that the leucine was
751 present in the Axin βcatBM-like urmetazoan and was lost in ctenophore Axin.
752 Subsequently, after splitting from an LCA with cnidarians, bilaterian Axin acquired the
753 critical histidine residue, and perhaps others, in the βcatBM-like sequence which
754 provided an increased affinity between Axin and β-catenin. These data help reveal the
755 molecular changes that occurred prior to the stabilization of Wnt/β-catenin regulation
756 that appears in the majority of bilaterian clades.

757

758 **Evolution of the bilaterian cWnt destruction complex**

759 The cWnt pathway is one of only two signal transduction pathways regulating
760 development that are restricted to all metazoans (Richards and Degnan 2009; Babonis

761 and Martindale 2017; Richter et al. 2018) and it plays diverse roles in cellular and
762 developmental processes and in homeostasis (Liu et al. 2002; MacDonald et al. 2009;
763 Petersen and Reddien 2009; Loh et al. 2016). One highly conserved function of the
764 cWnt pathway is its role in establishing the first embryonic axis in bilaterians (anterior-
765 posterior) and cnidarians (oral-aboral) (Wikramanayake et al. 2003; Petersen and
766 Reddien 2009; Loh et al. 2016; Holstein 2022). We and others have also shown that the
767 cWnt pathway also plays a critical role in segregating germ layers in cnidarians and
768 invertebrate bilaterians (Wikramanayake et al. 1998; Logan et al. 1999; Imai et al. 2000;
769 Wikramanayake et al. 2003; Henry et al. 2008; Darras et al. 2011; McCauley et al. 2015;
770 Holstein 2022). Considering the conservation of the role of cWnt signaling in these
771 fundamental processes it is remarkable how divergent the regulation of the cWnt
772 destruction complex appears to be between early branching metazoans and Bilateria.
773 Below, we suggest a model for the evolution of the cWnt DC that argues that the cWnt
774 DC in *Nematostella* is not "divergent" but it resembles the ancestral cWnt DC in the
775 cnidarian-bilaterian LCA that was functionally sufficient to regulate cWnt signaling in
776 animals that had relatively simple body plans. But this ancestral DC had promiscuous
777 interactions that increased the evolvability of the cWnt pathway during its broad
778 deployment as bilaterians underwent a massive radiation to evolve taxa with complex
779 body plans.

780 We know very little about cWnt signaling in ctenophores (Pang et al. 2010;
781 Walters et al. 2025) and it has also been difficult to study embryonic development in two
782 other early emerging taxa, poriferans and placozoans, due to the challenges in accessing
783 their embryos. Hence, our current focus has been on reconstructing the ancestral cWnt
784 DC in the cnidarian-bilaterian LCA, since we can experimental manipulate

785 *Nematostella* development and there is accumulated knowledge on the developmental
786 roles of the cWnt pathway in cnidarian development. We propose that the ancestral DC
787 that was present in the LCA of Bilateria and Cnidaria was scaffolded by an APC-like
788 protein that bound β-catenin and Axin, and an Axin protein that bound GSK-3β and had
789 two βcatBM-like sites that had low-affinity β-catenin-binding activity. This DC was
790 capable of regulating β-catenin stability in the cWnt pathway in the cnidarian-bilaterian
791 LCA. Whether this DC was able to directly target β-catenin for degradation through the
792 proteasome is not known at this time but regardless of the mechanism, it had to be very
793 different from how β-catenin is targeted for degradation in the bilaterian cWnt DC
794 (Roberts et al. 2011; Ranes et al. 2021).

795 Following the split of the bilaterians from the cnidarian-bilaterian LCA, the
796 βcatBM-like site at the C-terminus positioned between the GID and DAX domains of
797 bilaterian Axin gained amino acids that increased its affinity for β-catenin possibly by
798 gaining the functionally significant histidine residue seen in the bilaterian βcatBM
799 (Kremer et al. 2010). Likely in parallel, APC-like gained a long carboxy-terminal region
800 that led to the acquisition of redundant β-catenin and Axin-binding sites. In addition,
801 some bilaterian APC proteins gained domains that are involved in processes such as
802 oligomerization and interaction with microtubules (Nelson and Näthke 2013; Abbott
803 and Näthke 2023) (Fig. 8). The mechanism for domain addition to APC is unknown but
804 it is likely due to gene fusion since that is considered to be the predominant mechanism
805 for domain evolution in eukaryotic proteins and it generally occurs at the N- or C-
806 termini of proteins (Patthy 1999; Liu et al. 2005; Weiner et al. 2006).

807 We were unable to identify a βcatBM-like sequence in the Axin-RGS domain of
808 all the bilaterians we examined (listed in Table 1). This sequence was most likely lost

809 through drift, since with the acquisition of APC domains that interacted with high
810 affinity with the Axin RGS domain of the βcatBM-like sequence embedded in the RGS
811 would not have been able to interact with β-catenin if it had an earlier function in
812 binding β-catenin. The overall consequence of these changes may have been the
813 evolution of higher-affinity protein-protein interactions within the DC that allowed a
814 more efficient capture of free β-catenin from the cytoplasm and an increased level of
815 redundancy for β-catenin sequestration that served to buffer this critical regulatory
816 module from misregulation (Peterson-Nedry et al. 2008; Roberts et al. 2011) (Fig. 8C).
817 This idea is consistent with modeling studies which have shown that signaling pathways
818 evolve increased levels of complexity under standard evolutionary conditions, and this
819 complexity also provides increased robustness (Soyer and Bonhoeffer 2006). It is also
820 likely that the increased number of interfaces provided by the bilaterian Axin and APC
821 proteins provided additional targets for context-dependent regulation of the cWnt DC
822 during the evolution of complex body plans in the Bilateria. In conclusion, we suggest
823 that the cnidarian-bilaterian LCA cWnt DC had promiscuous protein interactions that
824 may have increased the evolvability of the cWnt pathway during its broad deployment
825 during bilaterian development and evolution. We believe that the approach we have
826 taken in this study illustrate the power of leveraging biodiversity to gain insight into the
827 evolution of protein function and protein-protein interactions networks that regulate
828 evolution and development.
829

830 **Materials and Methods**

831 *Animal care, spawning and culture*

832 Adult *N. vectensis* were spawned and eggs prepared for microinjections as
833 previously described (Wijesena et al. 2022).
834 Adult *Lytechinus variegatus* (Lv) were obtained from Duke University Marine
835 Lab (Beaufort, NC) or Pelagic Corporation (Sugarloaf Key, FL). Spawning of animals
836 and collection and treatments of gametes was done as previously described (Byrum et al.
837 2009; Sun et al. 2021).
838
839 *Cloning full length NvAxin and Reverse Transcriptase-PCR analysis*
840 Full length *N. vectensis* Axin (NvAxin) cDNA was PCR-amplified from egg stage
841 using primers designed against the NvAxin sequence (NEMVEDRAFT_v1g182113). The
842 primer sequences were: NvAxin FL forward primer:
843 CGCGCGGATCCATGAGCGAAGAGTTGTGTAG, and NvAxin FL reverse primer:
844 CGACCATCGATTGAGTCTACTTTTTCTACTTTGC. Egg, cleavage, blastula, gastrula and
845 planula stage embryos were collected separately for RNA extraction using Trizol reagent
846 (cat# 15596026, Invitrogen). Approximately 1 μg of total RNA was used for cDNA
847 synthesis using SuperScript IV first strand synthesis system (cat# 18091200,
848 Invitrogen). For PCR, NvAxin cDNA was amplified from different stage embryos. The
849 primers used to amplify NvAxin for RT-PCR were: NvAxin FP:
850 ATGAGCGAAGAGTTGTGTAG, and NvAxin RP: CGTGCATCTTGCTCGTCGTG.
851 The PCR procedures followed the protocol provided with the Q5 high fidelity
852 DNA polymerase kit (cat# M0491, NEB) with thermal cycling conditions, 98°C for 30
853 seconds, 35 cycles with (98°C 10 seconds, 62°C 30 seconds, 72°C 20-30 seconds/kb)
854 and 72°C for 2 minutes. The wildtype NvAxin was inserted into the GFP-pCS2^{+} vector
855 by BamH1 and Cla1 restriction enzyme digestion and ligation with T4 DNA ligase.

856

857 *Making NvAxin domain deletion constructs by site-directed mutagenesis*

858 NvAxinΔRGS, NvAxinΔGID, NvAxinΔDAX constructs were made using the Q5 Site-
859 directed mutagenesis kit (E0554, NEB). Primers were designed to delete the RGS, GID
860 and DAX domains separately. The following primer sequences were used: NvAxin
861 ΔRGS forward primer, CAGGCTCACAGAGACACC, and NvAxin ΔRGS reverse primer,
862 GAGTTAGCCCATCGCTCG; NvAxin ΔGID forward primer,
863 TGAGAGTGAATATGGCCAG, and NvAxin ΔGID reverse primer,
864 GGATTTTTGGCTTCCTTTG; NvAxinΔDAX forward primer,
865 CAATCGATTCGAATTCAAG, and NvAxinΔDAX reverse primer,
866 TTGTGTTTCTCCTTTTTCC. To perform the PCR procedure, the NvAxin-GFP pCS2+
867 plasmid was mixed with pairs of primers, the Q5 hot start high-fidelity 2X master mix
868 and nuclease free water to perform PCR procedure, followed by kinase, ligase & Dpnl
869 (KLD) treatment.

870

871 *Microinjection of morpholino antisense oligonucleotides and mRNAs*

872 For knockdown experiments, morpholino antisense oligonucleotides to Axin or APC-like
873 (NvAxin MO or NvAPC MO) and a standard control morpholino (Control MO) to a
874 random nucleotide sequence (5'-CCTCTTACCTCAGTTACAATTTATA-3') were
875 synthesized at Gene Tools, LLC (Eugene, OR). The NvAxin MO:
876 TACACAACTCTTCGCTCATCTCACG or NvAPC-like MO:
877 ATCCTCTTCAAAATCGTCCATGTTG were designed to span the start codon of the Axin
878 or APC-like transcripts. Each MO was injected at a final concentration of 2 mM in 30-
879 40% glycerol and dextran rhodamine 0.2 μg/μl (D1824, Invitrogen).

880 For overexpression experiments in *N. vectensis* or *L. variegatus*, the NvAxin-
881 GFP, NvAxin ΔRGS-GFP, NvAxin ΔGID-GFP, NvAxin ΔDIX-GFP, SpAxin-GFP, Nvβ-
882 catenin-mCherry, and Spβ-catenin-mCherry, NvAxin GID-GFP, and a control GFP
883 mRNA were all cloned into the pCS2+ vector. The pCS2+ vectors containing the
884 respective cDNAs were linearized with NotI and mRNA was transcribed using the SP6
885 mMessage mMachine Kit (Ambion® ThermoFisher Scientific). Dominant negative
886 NvTcf (NvdnTCF) (Röttinger et al. 2012) was used for downregulating cWNT signaling .
887 This construct was in the Venus-pDEST expression vector. The dnTCF-Venus construct
888 was linearized with Acc65I and *in vitro* transcribed as previously described (Röttinger et
889 al. 2012). The mRNAs were mixed in 40% glycerol to a final concentration of 0.5 µg/µl.
890 *GFP* mRNA was overexpressed as a control at the same molar ratio as previously
891 described (Bince and Wikramanayake 2008).
892 For co-overexpression experiments in *N. vectensis* or *L. variegatus*, *NvAxin-*
893 *GFP*, *NvAxin ΔGID-GFP*, *SpAxin-GFP*, *Nvβ-catenin-mCherry*, *Spβ-catenin-mCherry*
894 mRNAs were injected at a final concentration of 0.5 µg/µl, 0.5 µg/µl, 0.5 µg/µl, 0.2
895 µg/µl, 0.2 µg/µl respectively in 40% glycerol.
896 For each experiment, more than 100 embryos were injected per MO or per
897 mRNA. The experiments were repeated at least three times for biological replication
898 (Sun et al. 2021; Wijesena et al. 2022).
899
900 *CRISPR/Cas9 mediated knockouts and microinjections*
901 To knock out *NvAxin* or *NvAPC-lik*e, the synthetic guide RNAs (sgRNA;
902 Synthego, Inc.) and Cas9 complex (RNP complex) were introduced into *N. vectensis*
903 embryos by microinjection into zygotes. The *NvAxin* or *NvAPC-like* single guide RNAs

904 were designed using CRISPRscan and CHOPCHOP as previously described (Salinas-
905 Saavedra et al. 2018). Each single guide RNA was resuspended to 50 μM and stored at
906 −80°C. Cas9 was obtained from PNA bio (Cat.# CP01). Cas9 was reconstituted to 5 mM
907 and was aliquoted for single use and stored at −80°C.
908 A mixture (2.5 μl) containing sgRNA (12 μM), Cas9 (0.6mM), 40% Glycerol,
909 dextran rhodamine (0.2 μg/μl) and nuclease free H_2O was prepared and 1 μl of mixture
910 was loaded into needles for microinjection. The same amount of Cas9 only was injected
911 as a control. *NvAxin* sgRNA was used to introduce mutations into *NvAxin*, and *NvAPC-*
912 *like* sgRNA was used to introduce mutations into *NvAPC-like*, and the mixture of
913 *NvAxin* and *NvAPC-like* sgRNAs were used to mutate both genes in single embryos.
914
915 *Genomic DNA extraction from single embryos and validation of DNA editing by*
916 *CRISPR/Cas9*
917 Single *NvAxin* gRNA injected embryos were collected into 0.2 ml PCR tubes and
918 lysed by adding 20 μl of extraction buffer for 100 μl buffer: 1 μl 1M Tris, pH8.0; 0.3 μl
919 Tween 20; 0.2 μl 0.5M EDTA; 5 μl 1M KCl; 0.3 μl NP40; 2.5 μl proteinase K (20
920 mg/ml); nuclease free water). The tubes with lysed embryos were incubated for 3 hr at
921 55°C in a thermal cycler with periodic vortexing and the reaction was inactivated by
922 heating the tubes at 98°C for 5min. For the PCR analysis of *NvAxin* gRNA injected
923 embryos, 5 μl of genomic DNA was used as a template to carry out the PCR reaction as
924 described above for NvAxin cloning and then the amplicon was gel extracted, purified
925 and sequenced at Eurofins Scientific. The following primers were used to generate the
926 NvAxin amplicons from genomic DNA from embryos edited with the *NvAxin* gRNA:

927 forward primer: ATGGCCAGTCTAAAAAGTCTATCC, and reverse primer:
928 CTGGTGGTTCAATGTCAAGAACGGTAT.
929
930 *Quantitative PCR (qPCR)*
931 To evaluate the effects of injected gRNAs, MO or mRNA on lineage-specific gene
932 expression, quantitative PCR (qPCR) was performed on *N. vectensis*, or *L. variegatus*
933 cDNA samples synthesized from total RNA that was extracted from gRNA-, morpholino-
934 or mRNA-injected embryos. The control and treated samples were collected at the
935 blastula stage; *N. vectensis* embryos were at 24 hpf at 17°C and *L. variegatus* embryos
936 were at 6 hpf at 25°C. Total RNA was isolated using the Trizol reagent solution (cat#
937 AM9738, Invitrogen). The cDNA was synthesized from 50 -100 ng total RNA of control
938 and experimental embryos respectively using the qScript cDNA Synthesis kit (Quanta
939 Biosciences, Beverly). The PerfeCTa SYBR Green FastMix (Quanta Biosciences,
940 Beverly) was used for assembling the qPCR reactions. Each experiment was repeated 3
941 times with separate batches of embryos and each PCR reaction was done in triplicate.
942 The expression of selected genes was analyzed using the delta delta Ct ($2^{-\Delta\Delta Ct}$)
943 method and using GADPH as a control as previously described (Sun et al. 2021).
944 Statistical significance was determined using the Unpaired t test without specific fold
945 change cut off. The values represent the fold change relative to control. All the *L.*
946 *variegatus* primer sequences were obtained from David McClay's laboratory at Duke
947 University.
948
949 *Whole mount in situ hybridization (WMISH)*

950 *NvAxin* expression during early development was determined using whole
951 mount in situ hybridization (WMISH). The *NvAxin* in situ hybridization probe was
952 made using a pair of primers specifically targeting NvAxin: NvAxin-F: 5'
953 CGAAGGTAGAGCCGTATC 3', and NvAxin-R:
954 ATTTAGGTGACACTATAGGTCCGTCAGAGCATCACT, and was designed to contain an
955 Sp6 promoter for *in vitro* RNA synthesis. Embryo fixation and WMISH were performed
956 as previously described (Salinas-Saavedra et al. 2018). Embryos were fixed in 4%
957 paraformaldehyde with 0.2% glutaraldehyde in PTw (1XPBS+ 0.1%Tween-20) for 2 min
958 at room temperature, and then fixed in 4% paraformaldehyde in PTw for 1 hr at 4 °C. In
959 each experiment, a final concentration of 1 ng/µL anti-sense *NvAxin* probe was used
960 which was hybridized at 63°C for 2 days. *NvAxin* expression was detected using
961 NBT/BCIP as a substrate for the alkaline phosphatase conjugated to anti-digoxigenin
962 fab fragments (1:5000; Roche).
963
964 *F-actin and nuclear staining*
965 The morphology of *dnTcf-*, *NvAxin-*, *SpAxin-* and control *GFP*-RNA injected
966 embryos was examined using embryos collected at late gastrula stage (48 hpf at room
967 temperature) that were fixed and stained for F-actin and nuclear staining. Embryos
968 were collected and fixed as previously described with modifications (Salinas-Saavedra et
969 al. 2018). Briefly, embryos were first fixed in fix1 (100 mM HEPES pH 6.9; 0.05 M
970 EGTA; 5 mM MgSO4; 200 mM NaCl; 1x PBS; 3.7% Formaldehyde; 0.2%
971 Glutaraldehyde; 0.5% Triton X-100; and autoclaved ultrapure water) for 2-3 minutes
972 and then fixed in fix2 (100 mM HEPES pH 6.9; 0.05 M EGTA; 5 mM MgSO4; 200 mM
973 NaCl; 1x PBS; 3.7% Formaldehyde; 0.05% Glutaraldehyde; 0.5% Triton X-100; and

974 autoclaved ultrapure water) for one hour at room temperature on the rocker. Fixed
975 embryos were rinsed in PBT (X% Tween 20 in 1 x PBS, pH7.4) for 30 mins x 4 times.
976 Embryos were blocked with 5% normal sheep in PBT buffer for 1 hour at room
977 temperature on the rocker then rinsed with PBT for 30 mins x 4 times. For the F-actin
978 staining, embryos were stained with Phalloidin in PBT for 1 hour and then rinsed with
979 PBT for 10 min x 2 times. For nuclear staining, embryos were incubated in DAPI in PBT
980 for 1 hour and then rinsed in 1xPBS (PH 7.4) for 10 min x 3 times. Following these
981 washes, the embryos were dehydrated using a gradient of isopropanol (50, 75, 90, 100%,
982 100%). The embryos were then cleared with 1:2 benzyl benzoate: benzyl alcohol
983 (BB:BA) for 1 min x 2 times and mounted in BB:BA for imaging using scanning confocal
984 microscopy.
985
986 *In vitro Transcription and Translation (TNT) and Western blot analysis*
987 All GFP, mCherry, Flag and their fused constructs were in vitro transcribed and
988 translated using the TnT® Quick Coupled Transcription/Translation System with SP6
989 RNA polymerase promoter respectively (cat # L2080, Promega). Plasmids (at 1 μg
990 each) containing the respective cDNAs coding for the various fusion proteins were
991 incubated with TNT quick master mix at 30°C for 90 minutes. Protein expression was
992 examined using Western blot analysis with anti-GFP (cat# sc9996), anti-mCherry
993 antibodies (PA5-34974) or anti-flag (cat# 740001) respectively.
994 Protein-protein interaction was tested using ChromoTek GFP-Trap® Magnetic
995 Agarose following instructions to perform immunoprecipitation (IP) assay (cat # gtma,
996 Proteintech Group, INC., Rosemont, IL). Denatured IP protein samples were examined

997 on an 8% SDS-PAGE gel followed by Western blot analysis. Western blot was done as
998 previously described (Sun et al. 2024).
999
1000 *Split luciferase assay*
1001 N- and C-terminal fragments of click beetle green (CBG) split luciferase,
1002 including polypeptide linkers, were amplified and blunt-end-ligated into pSPE3-RfA
1003 vectors in a single restriction-ligation reaction. Coding sequences for *N. vectensis* and S.
1004 *purpuratus* Axin and β-catenin were cloned into pENTR using D-TOPO cloning kit
1005 (Invitrogen K240020) and recombined into CBG-tagged destination vectors via
1006 Gateway cloning (Invitrogen 11791020). Nanoluciferase (NanoLuc) was similarly cloned
1007 and recombined into pSPE3-RfA.
1008 Recombined Axin and β-catenin constructs were linearized, purified, and used for
1009 in vitro mRNA synthesis (Invitrogen AM1348). Equimolar CBG-tagged *Axin* and *β-*
1010 *catenin* mRNA mixtures, along with NanoLuc mRNA and fluorescent dextran, were
1011 microinjected into *Nematostella* zygotes. At 28 hours post-fertilization(hpf), live
1012 embryos were collected, and luminescence was measured after adding D-luciferin
1013 substrate (Goldbio LUCNA-100). Embryos were then lysed with ONE-Glo EX
1014 Luciferase Assay Reagent (Promega N1610), and further measurements were taken.
1015 NanoDLR Stop & Glo Reagent (Promega N1610) was used to stop the CBG reaction and
1016 initiate NanoLuc luminescence. NanoLuc signal was used to normalize protein levels
1017 and CBG intensities. Average NanoLuc signal from 15-20 minutes after the addition of
1018 substrate was used to determine ratios of protein levels. Average relative intensities
1019 across timepoints were calculated for each construct combination.
1020 Primers:

1021

Name	Sequence
linker-N-luc Fw	CAGATCTCGTACGCGTCCC
N-luc Rev	TTAGCCGTCGTCGTCGAT
Kozak-CBG-C-linker Fw	CAGAAAAAATGAAGGGTTATGTCAATAACGTTG
C-luc-linker Rev	TCCGCCCCGGGACG
NvAxin Fw	CACCATGAGCGAAGAGTTGTGTAG
NvAxin Rev	TGAGTCTACTTTTTCTACTTTGC
NvBeta-catenin Fw	CACCATGGGGATGCAGCAGGG
NvBeta-catenin-STOP Rev	TCAGAGGTCTGTGTCATACAGAG
SpAxin Fw	CACCATGAGTCTAGAAGTGTATAGG
SpAxin Rev	GTGATCATCGACAGATTC
SpBeta-catenin Fw	CACCATGGAGCAGGCAAGGTAC
SpBeta-catenin-STOP Rev	TTACAGATCGGTATCAAAGAACG
NanoLuc Fw	CACCATGGTCTTCACACTCG
NanoLuc Rev	TTACGCCAGAATGCG

1022

1023

1024 *AlphaFold 3 Protein-Protein interaction prediction*

1025 Computational methods were used to predict protein-protein interactions among
1026 the components of the β-catenin destruction complex in *S. purpuratus* (sea urchin) and
1027 *Nematostella*. Protein sequences for the individual components of the β-catenin

destruction complex were used as input in AlphaFold 3. The prediction accuracy was assessed using the predicted align error (PAE) and confidence scores such as the predicted TM-score (PTM) and inter-chain predicted TM-score (iPTM), which are indicators of the reliability of the predicted interactions. A PTM score above 0.5 indicates that the overall predicted fold for the complex may resemble the true structure. iPTM Values greater than 0.8 represent confident, high-quality predictions, while values below 0.5 suggest likely failed predictions. ipTM scores between 0.5 and 0.8 fall into an intermediate zone where predictions may be correct or incorrect21. AlphaFold 3 allowed for the visualization of possible binding interfaces and the determination of whether specific regions, such as the β-catenin binding domains, could facilitate protein-protein interactions, even in cases where canonical domains were not evident.

1042 References

1043 Abbott J, Näthke IS. 2023. The adenomatous polyposis coli protein 30 years on. *Semin Cell Dev*
1044 *Biol* 150–151:28–34.

1045 Adamska M, Larroux C, Adamski M, Green K, Lovas E, Koop D, Richards GS, Zwafink C,
1046 Degnan BM. 2010. Structure and expression of conserved Wnt pathway components in
1047 the demosponge Amphimedon queenslandica. *Evol Dev* 12:494–518.

1048 Babonis LS, Martindale MQ. 2017. Phylogenetic evidence for the modular evolution of
1049 metazoan signalling pathways. *Philosophical Transactions of the Royal Society B:*
1050 *Biological Sciences* 372:20150477.

1051 Bince JM, Wikramanayake AH. 2008. Functional analysis of Wnt signaling in the early sea
1052 urchin embryo using mRNA microinjection. *Methods Mol Biol* 469:213–222.

1053 Bryant P, Pozzati G, Elofsson A. 2022. Improved prediction of protein-protein interactions using
1054 AlphaFold2. *Nat Commun* 13:1265.

1055 Byrum CA, Xu R, Bince JM, McClay DR, Wikramanayake AH. 2009. Blocking Dishevelled
1056 signaling in the noncanonical Wnt pathway in sea urchins disrupts endoderm formation
1057 and spiculogenesis, but not secondary mesoderm formation. *Dev Dyn* 238:1649–1665.

1058 Chou H-Y, Howng S-L, Cheng T-S, Hsiao Y-L, Lieu A-S, Loh J-K, Hwang S-L, Lin C-C, Hsu
1059 C-M, Wang C, et al. 2006. GSKIP Is Homologous to the Axin GSK3β Interaction
1060 Domain and Functions as a Negative Regulator of GSK3β. *Biochemistry* 45:11379–
1061 11389.

1062 Dajani R, Fraser E, Roe SM, Yeo M, Good VM, Thompson V, Dale TC, Pearl LH. 2003.
1063 Structural basis for recruitment of glycogen synthase kinase 3β to the axin–APC scaffold
1064 complex. *EMBO J* 22:494–501.

1065 Darras S, Gerhart J, Terasaki M, Kirschner M, Lowe CJ. 2011. β-catenin specifies the
1066 endomesoderm and defines the posterior organizer of the hemichordate Saccoglossus
1067 kowalevskii. *Development* 138:959–970.

1068 Dunn CW, Hejnol A, Matus DQ, Pang K, Browne WE, Smith SA, Seaver E, Rouse GW, Obst
1069 M, Edgecombe GD, et al. 2008. Broad phylogenomic sampling improves resolution of
1070 the animal tree of life. *Nature* 452:745–749.

1071 Fagotto F, Jho E, Zeng L, Kurth T, Joos T, Kaufmann C, Costantini F. 1999. Domains of Axin
1072 Involved in Protein–Protein Interactions, Wnt Pathway Inhibition, and Intracellular
1073 Localization. *J Cell Biol* 145:741–756.

1074 Fodde R, Smits R, Clevers H. 2001. APC, Signal transduction and genetic instability in
1075 colorectal cancer. *Nat Rev Cancer* 1:55–67.

1076 Gammons M, Bienz M. 2018. Multiprotein complexes governing Wnt signal transduction. *Curr*
1077 *Opin Cell Biol* 51:42–49.

1078 Gerhart J. 1999. 1998 warkany lecture: Signaling pathways in development. *Teratology* 60:226–
1079 239.

1080 Ha N-C, Tonozuka T, Stamos JL, Choi H-J, Weis WI. 2004. Mechanism of phosphorylation-
1081 dependent binding of APC to beta-catenin and its role in beta-catenin degradation. *Mol*
1082 *Cell* 15:511–521.

1083 Hedgepeth CM, Deardorff MA, Rankin K, Klein PS. 1999. Regulation of glycogen synthase
1084 kinase 3beta and downstream Wnt signaling by axin. *Mol Cell Biol* 19:7147–7157.

1085 Henry JQ, Perry KJ, Wever J, Seaver E, Martindale MQ. 2008. β-Catenin is required for the
1086 establishment of vegetal embryonic fates in the nemertean, *Cerebratulus lacteus*.
1087 *Developmental Biology* 317:368–379.

1088 Holstein TW. 2022. The role of cnidarian developmental biology in unraveling axis formation
1089 and Wnt signaling. *Dev Biol* 487:74–98.

1090 Holzem M, Boutros M, Holstein TW. 2024. The origin and evolution of Wnt signalling. *Nat Rev*
1091 *Genet* 25:500–512.

1092 Houliston E, Leclère L, Munro C, Copley RR, Momose T. 2022. Past, present and future of
1093 *Clytia hemisphaerica* as a laboratory jellyfish. In: Goldstein B, Srivastava M, editors.
1094 Current Topics in Developmental Biology. Vol. 147. Emerging Model Systems in
1095 Developmental Biology. Academic Press. p. 121–151. Available from:
1096 https://www.sciencedirect.com/science/article/pii/S0070215321001046

1097 Ikeda S, Kishida S, Yamamoto H, Murai H, Koyama S, Kikuchi A. 1998. Axin, a negative
1098 regulator of the Wnt signaling pathway, forms a complex with GSK-3beta and beta-
1099 catenin and promotes GSK-3beta-dependent phosphorylation of beta-catenin. *EMBO J*
1100 17:1371–1384.

1101 Imai K, Takada N, Satoh N, Satou Y. 2000. β-catenin mediates the specification of endoderm
1102 cells in ascidian embryos. *Development* 127:3009–3020.

1103 Jumper J, Evans R, Pritzel A, Green T, Figurnov M, Ronneberger O, Tunyasuvunakool K, Bates
1104 R, Žídek A, Potapenko A, et al. 2021. Highly accurate protein structure prediction with
1105 AlphaFold. *Nature* 596:583–589.

1106 van Kappel EC, Maurice MM. 2017. Molecular regulation and pharmacological targeting of the
1107 β-catenin destruction complex. *Br J Pharmacol* 174:4575–4588.

1108 Kimelman D, Xu W. 2006. beta-catenin destruction complex: insights and questions from a
1109 structural perspective. *Oncogene* 25:7482–7491.

1110 Kinzler KW, Vogelstein B. 1996. Lessons from hereditary colorectal cancer. *Cell* 87:159–170.

1111 Kishida S, Yamamoto H, Ikeda S, Kishida M, Sakamoto I, Koyama S, Kikuchi A. 1998. Axin, a
1112 Negative Regulator of the Wnt Signaling Pathway, Directly Interacts with Adenomatous
1113 Polyposis Coli and Regulates the Stabilization of β-Catenin. *Journal of Biological*
1114 *Chemistry* 273:10823–10826.

1115 Kohler EM, Derungs A, Daum G, Behrens J, Schneikert J. 2008. Functional definition of the
1116 mutation cluster region of adenomatous polyposis coli in colorectal tumours. *Hum Mol*
1117 *Genet* 17:1978–1987.

1118 Kraus Y, Aman A, Technau U, Genikhovich G. 2016. Pre-bilaterian origin of the blastoporal
1119 axial organizer. *Nat Commun* 7:11694.

1120 Kremer SA, Erdeniz N, Peterson-Nedry W, Swanson EA, Wehrli M. 2010. In vivo analysis in
1121 Drosophila reveals differential requirements of contact residues in Axin for interactions
1122 with GSK3beta or beta-catenin. *Dev Biol* 337:110–123.

1123 Kumburegama S, Wijesena N, Xu R, Wikramanayake AH. 2011. Strabismus-mediated primary
1124 archenteron invagination is uncoupled from Wnt/β-catenin-dependent endoderm cell fate
1125 specification in Nematostella vectensis (Anthozoa, Cnidaria): Implications for the
1126 evolution of gastrulation. *EvoDevo* 2:2.

1127 Layden MJ, Rentzsch F, Röttinger E. 2016. The rise of the starlet sea anemone Nematostella
1128 vectensis as a model system to investigate development and regeneration. *Wiley*
1129 *Interdiscip Rev Dev Biol* 5:408–428.

1130 Lebedeva T, Aman AJ, Graf T, Niedermoser I, Zimmermann B, Kraus Y, Schatka M, Demilly
1131 A, Technau U, Genikhovich G. 2021. Cnidarian-bilaterian comparison reveals the
1132 ancestral regulatory logic of the β-catenin dependent axial patterning. *Nat Commun*
1133 12:4032.

1134 Lee PN, Kumburegama S, Marlow HQ, Martindale MQ, Wikramanayake AH. 2007.
1135 Asymmetric developmental potential along the animal-vegetal axis in the anthozoan
1136 cnidarian, Nematostella vectensis, is mediated by Dishevelled. *Dev Biol* 310:169–186.

1137 Liu C, Li Y, Semenov M, Han C, Baeg GH, Tan Y, Zhang Z, Lin X, He X. 2002. Control of
1138 beta-catenin phosphorylation/degradation by a dual-kinase mechanism. *Cell* 108:837–
1139 847.

1140 Liu J, Xiao Q, Xiao J, Niu C, Li Y, Zhang X, Zhou Z, Shu G, Yin G. 2022. Wnt/β-catenin
1141 signalling: function, biological mechanisms, and therapeutic opportunities. *Sig Transduct*
1142 *Target Ther* 7:1–23.

1143 Liu M, Walch H, Wu S, Grigoriev A. 2005. Significant expansion of exon-bordering protein
1144 domains during animal proteome evolution. *Nucleic Acids Research* 33:95–105.

1145 Logan CY, Miller JR, Ferkowicz MJ, McClay DR. 1999. Nuclear β-catenin is required to specify
1146 vegetal cell fates in the sea urchin embryo. *Development* 126:345–357.

1147 Loh KM, van Amerongen R, Nusse R. 2016. Generating Cellular Diversity and Spatial Form:
1148 Wnt Signaling and the Evolution of Multicellular Animals. *Dev Cell* 38:643–655.

1149 MacDonald BT, Tamai K, He X. 2009. Wnt/β-Catenin Signaling: Components, Mechanisms,
1150 and Diseases. *Developmental Cell* 17:9–26.

1151 McCauley BS, Akyar E, Saad HR, Hinman VF. 2015. Dose-dependent nuclear β-catenin
1152 response segregates endomesoderm along the sea star primary axis. *Development*
1153 142:207–217.

1154 Mendoza-Topaz C, Mieszczanek J, Bienz M. 2011. The Adenomatous polyposis coli tumour
1155 suppressor is essential for Axin complex assembly and function and opposes Axin's
1156 interaction with Dishevelled. *Open Biol* 1:110013.

1157 Meng EC, Goddard TD, Pettersen EF, Couch GS, Pearson ZJ, Morris JH, Ferrin TE. 2023.
1158 UCSF ChimeraX: Tools for structure building and analysis. *Protein Sci* 32:e4792.

1159 Momose T, Derelle R, Houliston E. 2008. A maternally localised Wnt ligand required for axial
1160 patterning in the cnidarian Clytia hemisphaerica. *Development* 135:2105–2113.

1161 Momose T, Houliston E. 2007. Two oppositely localised frizzled RNAs as axis determinants in a
1162 cnidarian embryo. *PLoS Biol* 5:e70.

1163 Nelson S, Näthke IS. 2013. Interactions and functions of the adenomatous polyposis coli (APC)
1164 protein at a glance. *Journal of Cell Science* 126:873–877.

1165 Pang K, Ryan JF, Mullikin JC, Baxevanis AD, Martindale MQ. 2010. Genomic insights into Wnt
1166 signaling in an early diverging metazoan, the ctenophore Mnemiopsis leidyi. *EvoDevo*
1167 1:10.

1168 Patthy L. 1999. Genome evolution and the evolution of exon-shuffling--a review. *Gene* 238:103–
1169 114.

1170 Petersen CP, Reddien PW. 2009. Wnt signaling and the polarity of the primary body axis. *Cell*
1171 139:1056–1068.

1172 Peterson-Nedry W, Erdeniz N, Kremer S, Yu J, Baig-Lewis S, Wehrli M. 2008. Unexpectedly
1173 robust assembly of the Axin destruction complex regulates Wnt/Wg signaling in
1174 Drosophila as revealed by analysis in vivo. *Dev Biol* 320:226–241.

1175 Pires-daSilva A, Sommer RJ. 2003. The evolution of signalling pathways in animal
1176 development. *Nat Rev Genet* 4:39–49.

1177 Polakis P. 1995. Mutations in the APC gene and their implications for protein structure and
1178 function. *Current Opinion in Genetics & Development* 5:66–71.

1179 Pronobis MI, Deuitch N, Posham V, Mimori-Kiyosue Y, Peifer M. 2017. Reconstituting
1180 regulation of the canonical Wnt pathway by engineering a minimal β-catenin destruction
1181 machine. *Mol Biol Cell* 28:41–53.

1182 Pronobis MI, Rusan NM, Peifer M. 2015. A novel GSK3-regulated APC:Axin interaction
1183 regulates Wnt signaling by driving a catalytic cycle of efficient βcatenin destruction.
1184 *eLife* [Internet]. Available from: https://elifesciences.org/articles/08022

1185 Qiu L, Sun Y, Ning H, Chen G, Zhao W, Gao Y. 2024. The scaffold protein AXIN1: gene
1186 ontology, signal network, and physiological function. *Cell Communication and Signaling*
1187 22:77.

1188 Ranes M, Zaleska M, Sakalas S, Knight R, Guettler S. 2021. Reconstitution of the destruction
1189 complex defines roles of AXIN polymers and APC in β-catenin capture, phosphorylation,
1190 and ubiquitylation. *Mol Cell* 81:3246-3261.e11.

1191 Richards GS, Degnan BM. 2009. The dawn of developmental signaling in the metazoa. *Cold*
1192 *Spring Harb Symp Quant Biol* 74:81–90.

1193 Richter DJ, Fozouni P, Eisen MB, King N. 2018. Gene family innovation, conservation and loss
1194 on the animal stem lineage.Telford MJ, editor. *eLife* 7:e34226.

1195 Richter DJ, King N. 2013. The genomic and cellular foundations of animal origins. *Annu Rev*
1196 *Genet* 47:509–537.

1197 Roberts DM, Pronobis MI, Poulton JS, Waldmann JD, Stephenson EM, Hanna S, Peifer M.
1198 2011. Deconstructing the ßcatenin destruction complex: mechanistic roles for the tumor
1199 suppressor APC in regulating Wnt signaling. *Mol Biol Cell* 22:1845–1863.

1200 Rokas A. 2008. The origins of multicellularity and the early history of the genetic toolkit for
1201 animal development. *Annu Rev Genet* 42:235–251.

1202 Ros-Rocher N, Pérez-Posada A, Leger MM, Ruiz-Trillo I. 2021. The origin of animals: an
1203 ancestral reconstruction of the unicellular-to-multicellular transition. *Open Biol*
1204 11:200359.

1205 Röttinger E, Dahlin P, Martindale MQ. 2012. A Framework for the Establishment of a Cnidarian
1206 Gene Regulatory Network for "Endomesoderm" Specification: The Inputs of ß-
1207 Catenin/TCF Signaling. *PLOS Genetics* 8:e1003164.

1208 Salinas-Saavedra M, Rock AQ, Martindale MQ. 2018. Germ layer-specific regulation of cell
1209 polarity and adhesion gives insight into the evolution of mesoderm. *Elife* 7:e36740.

1210 Schneider SQ, Finnerty JR, Martindale MQ. 2003. Protein evolution: structure-function
1211 relationships of the oncogene beta-catenin in the evolution of multicellular animals. *J Exp*
1212 *Zool B Mol Dev Evol* 295:25–44.

1213 Schneikert J, Behrens J. 2007. The canonical Wnt signalling pathway and its APC partner in
1214 colon cancer development. *Gut* 56:417–425.

1215 Schultz DT, Haddock SHD, Bredeson JV, Green RE, Simakov O, Rokhsar DS. 2023. Ancient
1216 gene linkages support ctenophores as sister to other animals. *Nature* 618:110–117.

1217 Servetnick MD, Steinworth B, Babonis LS, Simmons D, Salinas-Saavedra M, Martindale MQ.
1218 2017. Cas9-mediated excision of Nematostella brachyury disrupts endoderm
1219 development, pharynx formation and oral-aboral patterning. *Development* 144:2951–
1220 2960.

1221 Shor B, Schneidman-Duhovny D. 2024. CombFold: predicting structures of large protein
1222 assemblies using a combinatorial assembly algorithm and AlphaFold2. *Nat Methods*
1223 21:477–487.

1224 Soyer OS, Bonhoeffer S. 2006. Evolution of complexity in signaling pathways. *Proceedings of*
1225 *the National Academy of Sciences* 103:16337–16342.

1226 Stamos JL, Weis WI. 2013. The β-catenin destruction complex. *Cold Spring Harb Perspect Biol*
1227 5:a007898.

1228 Sun H, Peng CJ, Wang L, Feng H, Wikramanayake AH. 2021. An early global role for Axin is
1229 required for correct patterning of the anterior-posterior axis in the sea urchin embryo.
1230 *Development* 148:dev191197.

1231 Sun H, Shami Shah A, Chiu D-C, Bonfini A, Buchon N, Baskin JM. 2024. Wnt/β-catenin
1232 signaling within multiple cell types dependent upon kramer regulates Drosophila
1233 intestinal stem cell proliferation. *iScience* 27:110113.

1234 Valenta T, Hausmann G, Basler K. 2012. The many faces and functions of β-catenin. *EMBO J*
1235 31:2714–2736.

1236 Villalobos V, Naik S, Bruinsma M, Dothager RS, Pan M-H, Samrakandi M, Moss B, Elhammali
1237 A, Piwnica-Worms D. 2010. Dual-Color Click Beetle Luciferase Heteroprotein Fragment
1238 Complementation Assays. *Chem Biol* 17:1018–1029.

1239 Walters BM, Guttieres LJ, Goëb M, Marjenberg SJ, Martindale MQ, Wikramanayake AH. 2024.
1240 β-catenin localization in the ctenophore Mnemiopsis leidyi suggests an ancestral role in
1241 cell adhesion and nuclear function. :2024.08.29.610370. Available from:
1242 https://www.biorxiv.org/content/10.1101/2024.08.29.610370v1

1243 Weiner J, Beaussart F, Bornberg-Bauer E. 2006. Domain deletions and substitutions in the
1244 modular protein evolution. *FEBS J* 273:2037–2047.

1245 Wijesena N, Sun H, Kumburegama S, Wikramanayake AH. 2022. Distinct Frizzled receptors
1246 independently mediate endomesoderm specification and primary archenteron
1247 invagination during gastrulation in *Nematostella*. *Developmental Biology* 481:215–225.

Wikramanayake AH, Hong M, Lee PN, Pang K, Byrum CA, Bince JM, Xu R, Martindale MQ. 2003. An ancient role for nuclear β-catenin in the evolution of axial polarity and germ layer segregation. *Nature* 426:446–450.

Wikramanayake AH, Huang L, Klein WH. 1998. β-Catenin is essential for patterning the maternally specified animal-vegetal axis in the sea urchin embryo. *Proceedings of the National Academy of Sciences* 95:9343–9348.

Xing Y, Clements WK, Kimelman D, Xu W. 2003. Crystal structure of a β-catenin/Axin complex suggests a mechanism for the β-catenin destruction complex. *Genes Dev.* 17:2753–2764.

Yang J, Zhang W, Evans PM, Chen X, He X, Liu C. 2006. Adenomatous polyposis coli (APC) differentially regulates beta-catenin phosphorylation and ubiquitination in colon cancer cells. *J Biol Chem* 281:17751–17757.

Acknowledgements and funding sources

This work was partially supported by NASA (80NSSC18K1067) to AHW and MQM and NSF (1755364) to MQM. We thank Ryan Christopher Vignogna, Lin Luan, and Le Li for help with AlphaFold analysis.

Figures

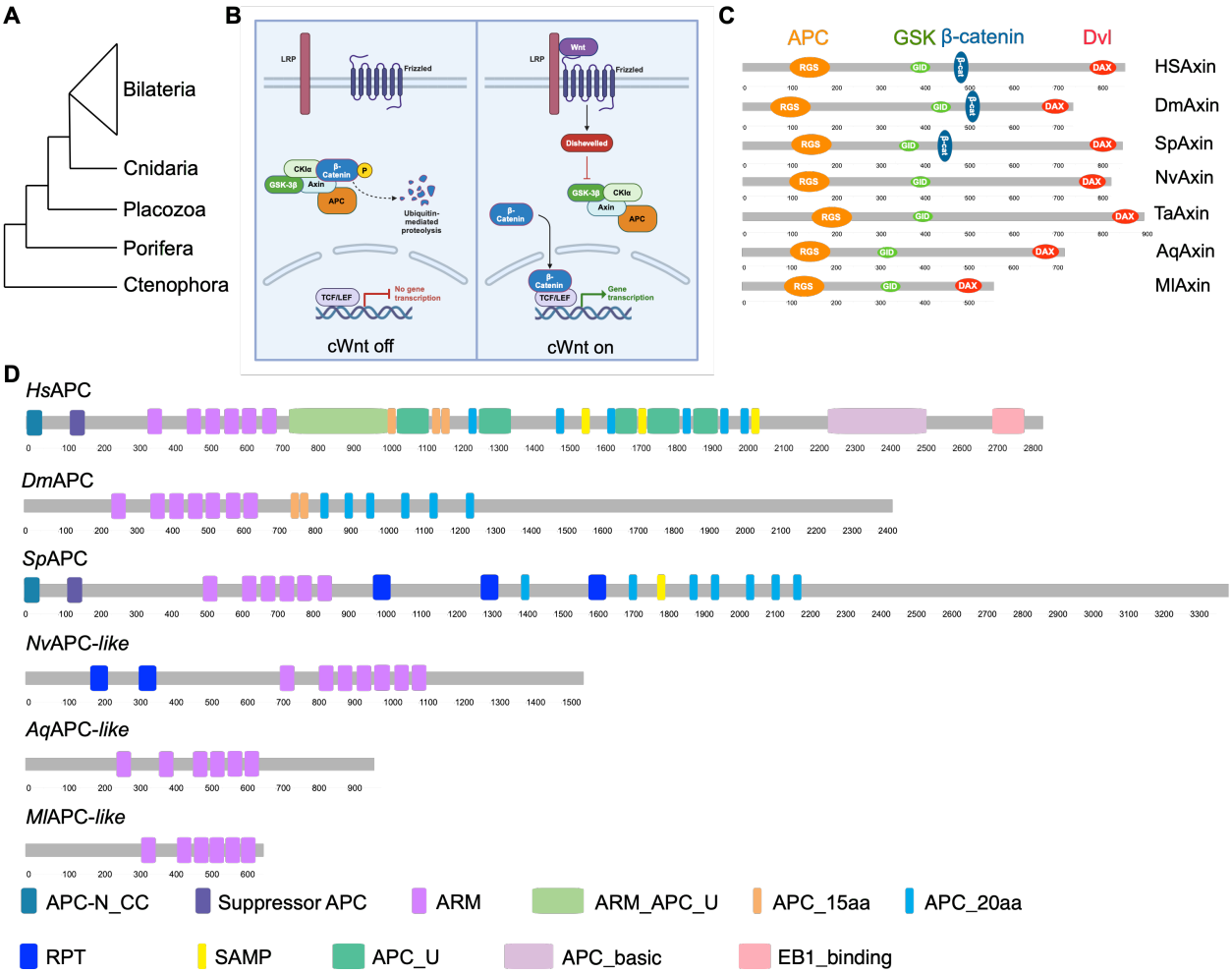

Figure 1- A phylogenetic overview perspective of the evolution of changes in protein-protein interaction domains in the Wnt/ β-catenin pathway destruction complex scaffolding proteins Axin and APC. (A) A simplified phylogenetic tree showing the evolutionary relationships between Bilateria and non-Bilateria taxa. (B) Simplified representation of the cWnt pathway in its "off "and "on" states, showing the activity of the destruction complex scaffolded by the Axin and APC proteins. (C) Schematic diagram comparing the main protein binding domains of Axin in bilaterians and non-bilaterians. (D) Schematic diagram of APC protein domain structures in bilaterians and non-bilaterians. *Hs*, *Homo sapiens*; *Dm*, *Drosophila melanogaster*; *Sp*, *Strongylocentrotus purpuratus*; *Nv*, *Nematostella vectensis*; *Ta*, *Trichoplax adhaerens*; *Aq*, *Amphimedon queenslandica*; *Ml*, *Mnemiopsis leidyi*. The numbers under the protein structures indicate the amino acid position. The color codes for the domains are indicated within or below the protein structures.

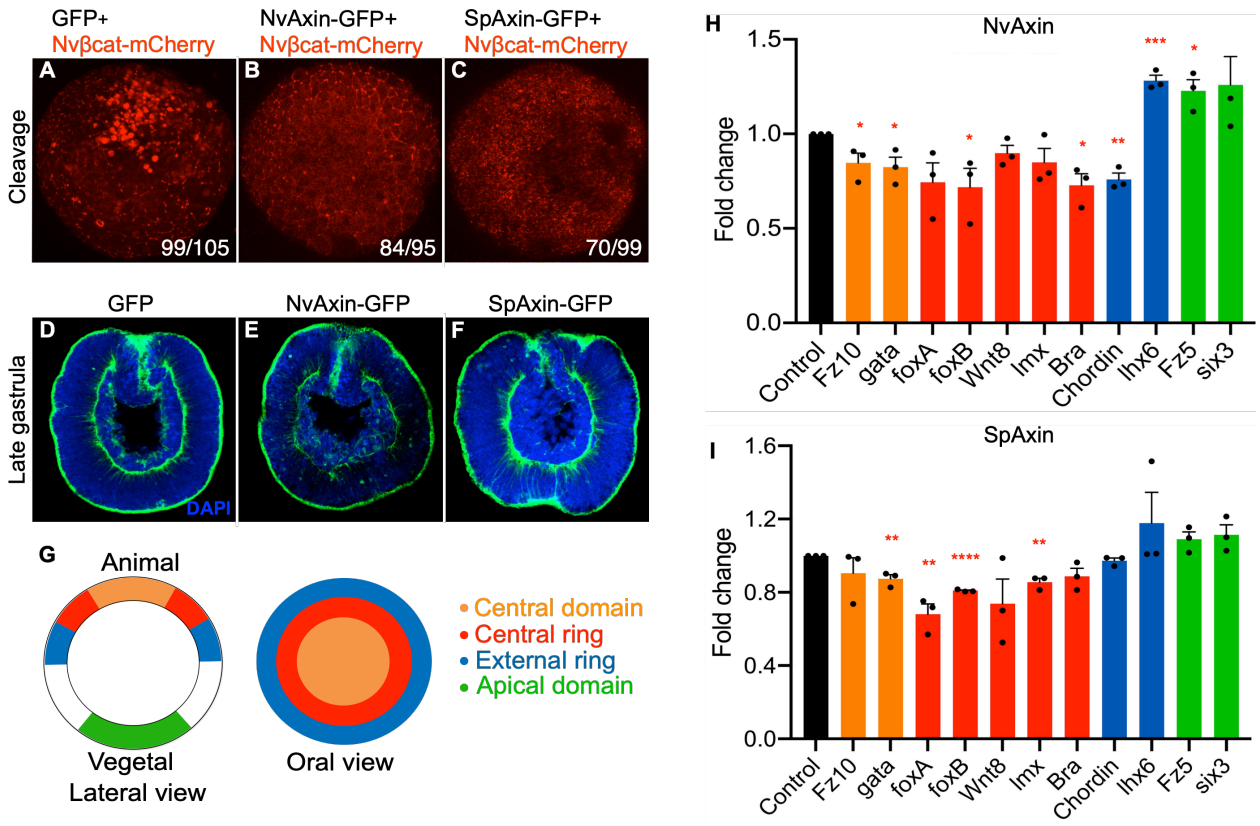

Figure 2- Overexpression of Axin in *Nematostella* embryos disrupts Wnt/β-catenin signaling. (A) Live imaging of embryos showed that in GFP and Nvβ-catenin-mCherry co-expressing embryos β-catenin-mCherry was enriched in the nuclei at one side of the embryo. However, co-overexpression of NvAxin-GFP (B) or SpAxin-GFP (C) with Nvβ-catenin-mCherry eliminated the nuclearization of β-catenin-mCherry. (D-F) Compared to GFP overexpressing control embryos which had a well-formed gut epithelium (D), NvAxin-GFP overexpressing embryos (E) and sea urchin Axin overexpressing embryos (SpAxin-GFP) (F) initiated primary invagination but failed to maintain a normal gut epithelium at the late gastrula stage. Green: phalloidin; Blue: DAPI. (G) Gene syn-expression domains as defined in Röttinger et al. (2012). Figure on the left shows a lateral view and the figure on the right shows the oral view. (H, I) qPCR analyses of NvAxin or SpAxin overexpressing embryos at 24 hpf (hours post fertilization) showed that all endomesoderm gene markers (orange, and red bars) and pharynx markers (blue bars) were downregulated, except for lhx6. The values represent the fold change relative to the GFP control (black bars). The qPCR experiments were replicated with three separate batches of embryos, with three technical replicates in each experiment. GAPDH was used as the internal control. Statistical significance was determined using the Unpaired t test. ****, $p<0.0001$; ***, $p<0.001$; **, $p<0.01$; *, $p<0.05$; n=3.

1331
1332

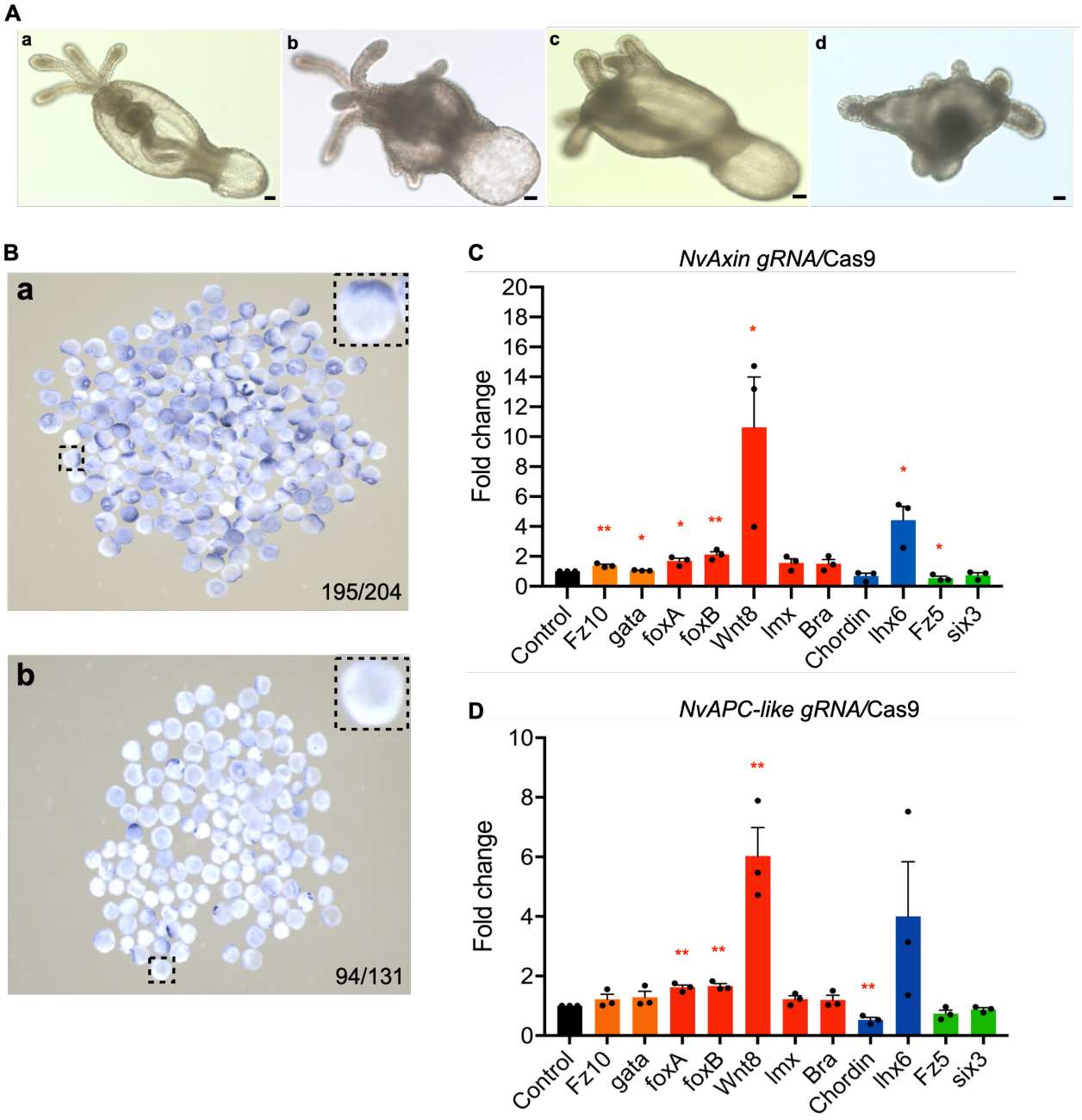

1333

1334 **Figure 3- CRISPR/Cas9 mediated knockout of *Axin* and *APC-like* induces**
1335 **ectopic tentacles and upregulates endomesoderm gene expression in**
1336 ***Nematostella* embryos.** (A) *Nematostella* 4-tentacle polyp, 7 days post-fertilization
1337 (7dpf) injected with Cas9 at the zygote stage (a). *NvAxin* guide RNA/Cas9-injected
1338 polyps produced ectopic tentacles (b), which is similar to what is seen in *NvAPC-like*
1339 gRNA/Cas9 injected polyps (c). Co-injection of *Axin* and *APC-like* gRNA/Cas9
1340 produced a more severe phenotype (d) than *Axin* or *APC-like* gRNA/Cas9 single

1341 injections. Scale bar = 20μm. For each injection experiment, 100-200 embryos were
1342 injected with either gRNA/Cas9 or Cas9 alone. Among these, 70-75% of the
1343 gRNA/Cas9-injected embryos and more than 95% Cas9 only injected embryos exhibited
1344 the same morphology as shown in the representative figures. (B) While Cas9-injected
1345 embryos have normal oral pole *Axin* localization (a, blue staining), in situ hybridization
1346 showed that *NvAxin*/Cas9 injected embryos displayed reduced *Axin* expression (b).
1347 WMISH showed that 81.9% of the control embryos showed strong *NvAxin* expression at
1348 the animal pole; 13.7% showed detectable but weaker asymmetrical *NvAxin* expression,
1349 and 4.4% showed no detectable signal (n=204) (Fig. 2Ba). By contrast, 72.5% of *NvAxin*
1350 gRNA/Cas9-injected embryos showed no detectable *Axin* expression, 24.4% showed
1351 weak *Axin* expression, and only 3.1% showed a signal like that seen in the control
1352 (n=131) (Fig. 2Bb). The embryos with weak *NvAxin* signals may be due to incomplete
1353 excision of *NvAxin* or the generation of mosaic embryos where the gene was only
1354 excised in some nuclei. (C and D) qPCR shows the effects of *Axin* and *APC-like* knock-
1355 out by CRISPR/Cas9 on the expression of endomesoderm and pharynx gene markers.
1356 *Fz10*, *gata*, *foxA*, *foxB*, *Wnt8*, *lmx*, *Brachyury (Bra)* (orange and red bars) are endo
1357 mesodermal markers, *Chordin*, *lhx6* (blue bars) are markers for the pharynx; *Fz5* and
1358 *six3* (green bars) are ectoderm gene makers. qPCR experiments were replicated with
1359 three separate batches of embryos with three technical replicates in each
1360 experiment. GAPDH was used as the internal control. Graphs shown fold change in
1361 mRNA levels normalized to the Cas9 only control (black bars). Statistical significance
1362 was determined using the Unpaired t test. **, $p<0.01$; *, $p<0.05$; n=3.

1363
1364

1365

1366

1367
1368
1369
1370
1371
1372
1373

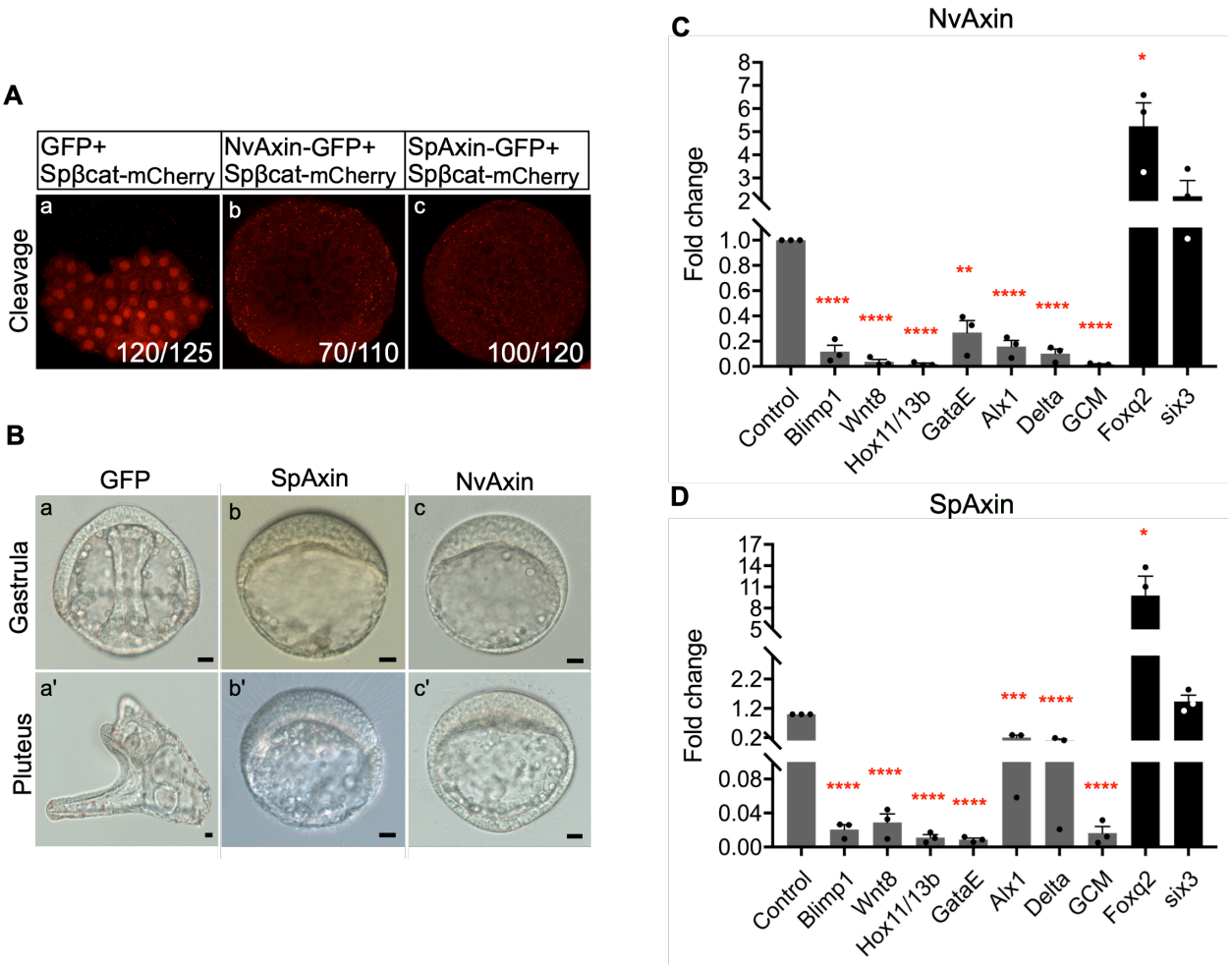

Figure 4- Overexpression of *Nematostella* Axin in sea urchin embryos blocks nuclearization of β-catenin and cWnt signaling. (A) In the control where GFP and Spβ-catenin-mCherry were co-expressed, β-catenin was enriched in the nuclei at the vegetal pole (a). Co-overexpression of NvAxin (b) or SpAxin (c) with Spβ-catenin-mCherry downregulated the nuclearization of β-catenin. (B) Control embryos injected with *GFP* mRNA developed normally (a, a'), while embryos developing from *SpAxin* or *NvAxin* mRNA-injected zygotes became severely anteriorized (b, b' and c, c'). Scale bar = 10μm. (C and D) qPCR analyses showed that NvAxin or SpAxin overexpressing embryos downregulated endomesoderm genes and upregulated neuroectoderm genes. The bar graph shows the fold change of each gene between *Axin* mRNA-injected and *GFP* mRNA-injected control embryos. *Blimp1*, *Wnt8*, *Hox11/13b*, *GataE*, *Alx1*, *Delta* and *GCM* are endomesoderm gene markers; *Foxq2* and *Six3* are neuroectoderm gene markers. qPCR experiments were replicated with three separate batches of embryos with three technical replicates in each experiment. GAPDH was used as the internal control. Statistical significance was determined using the Unpaired t test. ****, $p<0.0001$; ***, $p<0.001$; **, $p<0.01$; *, $p<0.05$; n=3. For each injection

experiment, 200-300 embryos were injected with each construct and more than 95% of embryos had the same morphology as shown in the representative figures.

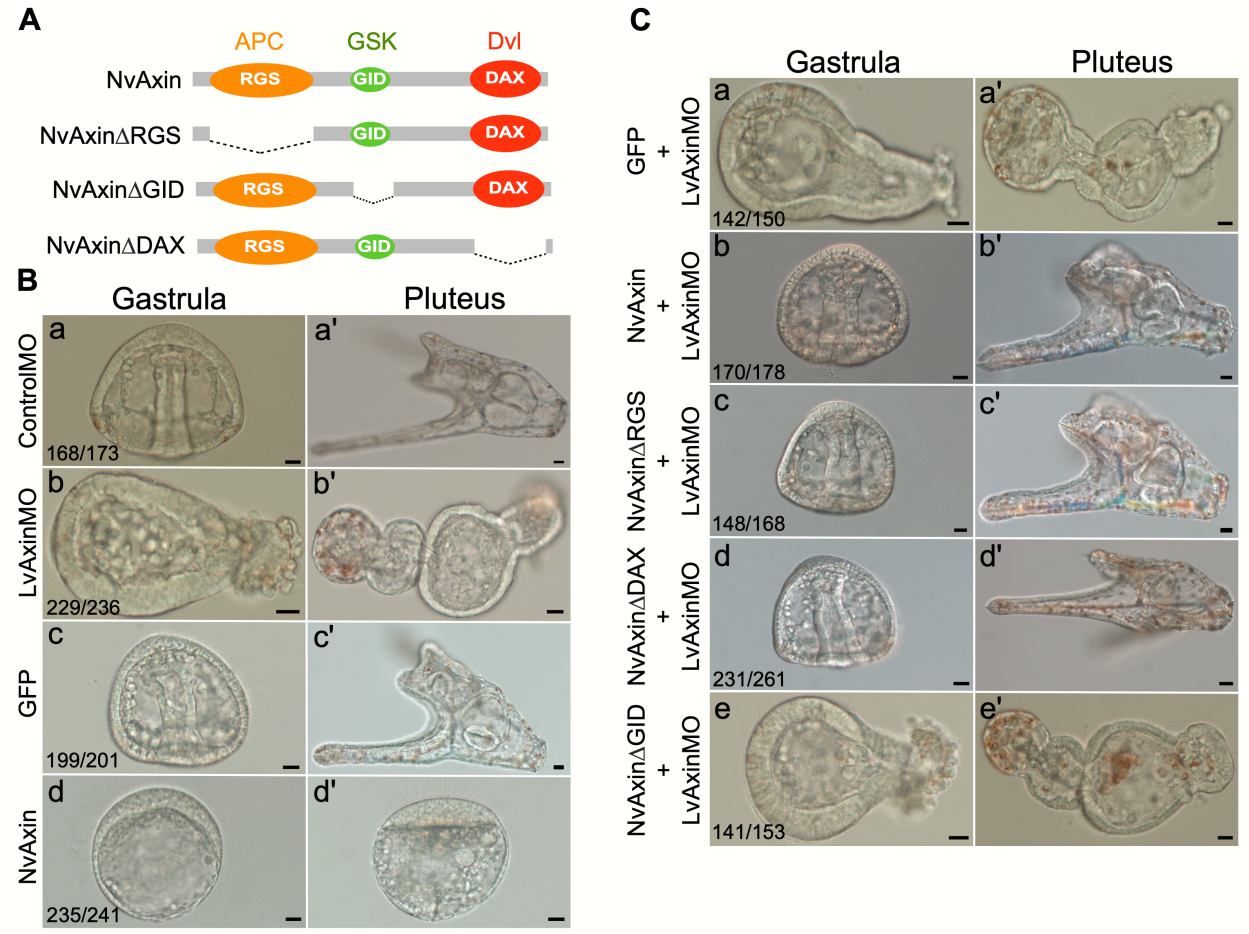

Figure 5- Sea urchin embryos posteriorized by Axin knock-down can be rescued by full-length NvAxin, NvAxinΔRGS, and NvAxinΔDAX, but not NvAxinΔGID. (A) Schematic representations of full-length Axin and single domain-deleted Axin constructs. (B) Gastrula and pluteus larva developing from Control MO, LvAxin MO, *GFP* mRNA or *NvAxin* mRNA injected zygotes from the sea urchin *Lytechinus variegatus* (a-d'). Control MO-injected embryos develop normally (a,a'), while LvAxin MO-injected embryos become posteriorized (b, b'). *GFP* mRNA-injected zygotes produce normal embryos (c, c'), while *NvAxin* mRNA-injected zygotes develop into anteriorized embryos (d, d'). (C) The posteriorized phenotype induced in LvAxin MO-injected embryos is not rescued by control *GFP* mRNA co-injection (a, a') but is rescued by the overexpression of NvAxin (b, b'), NvAxinΔRGS (c, c'), and NvAxinΔDAX (d, d'). Injection of *NvAxinΔGID* mRNA fails to rescue the posteriorization induced by Axin knockdown (e,e'). Scale bar = 10 µm. The numbers in the panels indicate the number of embryos examined and the number that showed the phenotype.

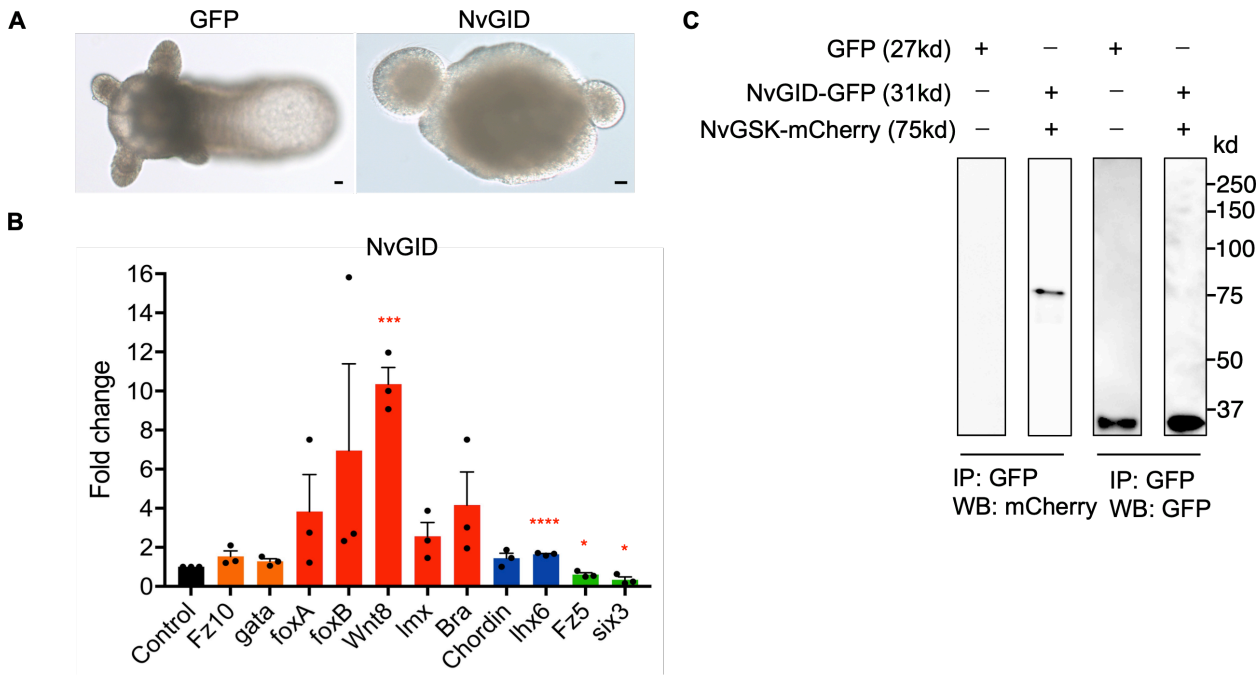

Figure 6- Overexpression of the NvAxin GID domain upregulated endomesodermal and pharyngeal gene expression in *Nematostella* embryos. (A) Comparison of animals developing from *Nematostella* zygotes injected with *GFP* mRNA (control) or *NvAxin-GID (NvGID)* mRNA at 7 days post fertilization (7dpf). At 7dpf control animals were at the polyp stage while *NvGID* RNA-injected embryos developed abnormally. Scale bar =10 µm. (B) qPCR analyses of NvGID overexpressing embryos at 24 hpf (hours post fertilization) showed that all endomesoderm gene markers (orange, red and blue bars) were upregulated. Some genes were unregulated at modest levels while others showed significant increases. The two apical domain genes were significantly downregulated. The qPCR experiments were replicated with three separate batches of embryos, with three technical replicates in each experiment. GAPDH was used as the internal control. Graphs shown fold change in mRNA levels normalized to the GFP control (black bars). Statistical significance was determined using the Unpaired t test. ****, $p<0.0001$; ***, $p<0.001$; *, $p<0.05$; n=3. (C) Western blot analysis of anti-GFP antibody-mediated immunoprecipitation of *in vitro* synthesized NvGID-GFP and NvGSK-3β-mCherry fused proteins.

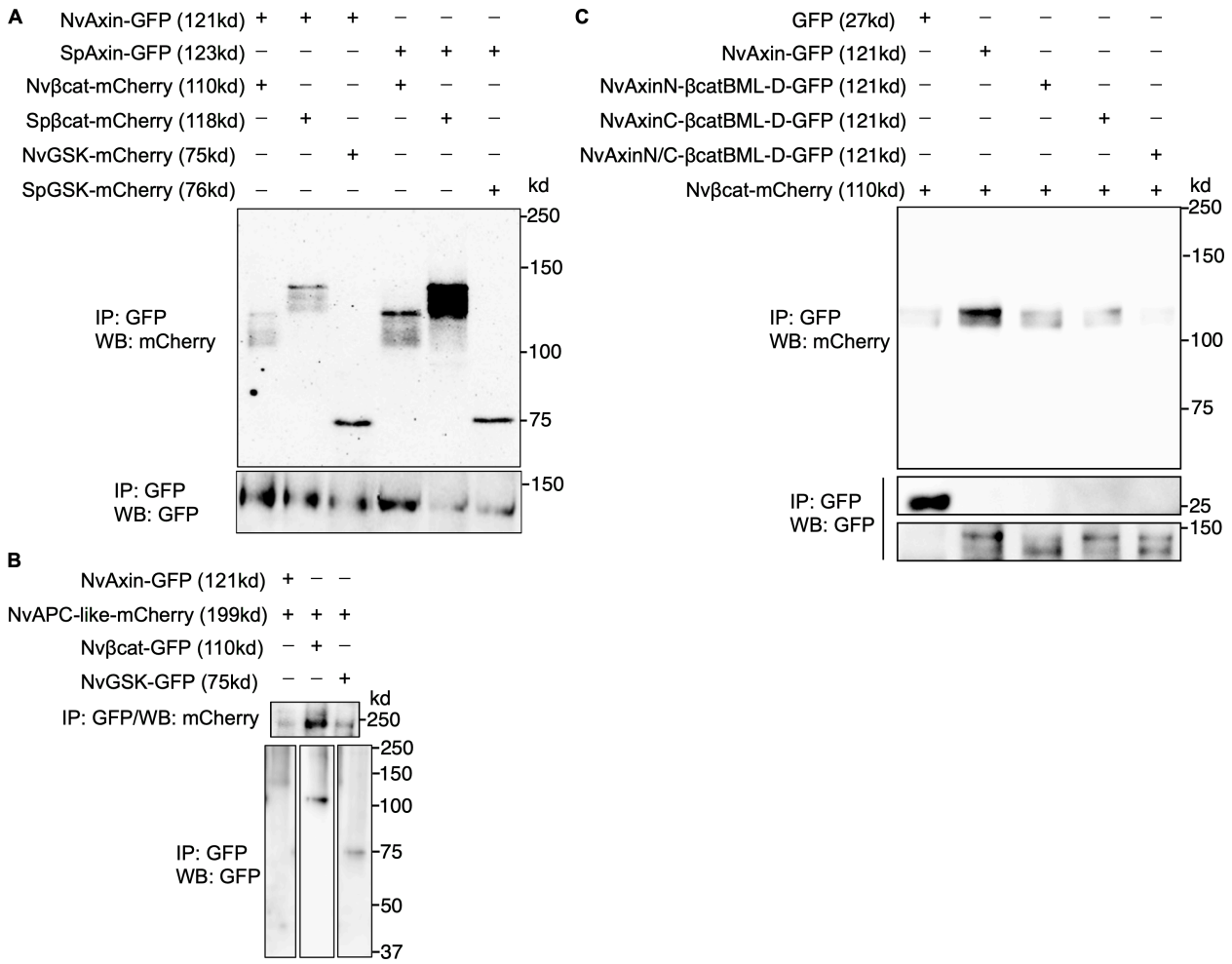

Figure 7- *In vitro* analysis of protein-protein interactions indicate direct interactions between Nvβ-catenin and components of the *Nematostella* β-catenin destruction complex. (A) *In vitro*-synthesized GFP- or mCherry-fused proteins were tested for potential interactions by mixing a GFP-fused partner with an mCherry-fused partner and performing immunoprecipitation (IP) with an anti-GFP antibody. The labels at the top of the panel show the interacting proteins in each experiment. The top part of the Western blot analysis shows the protein-protein interactions between protein pairs. The bottom part of the figure shows the Western blot of GFP-tagged proteins. Sea urchin (*Strongylocentrotus purpuratus*) β-catenin (Spβ-catenin) shows a strong interaction with sea urchin Axin (SpAxin) (Lane 5), while Nvβ-catenin shows a consistent but considerably weaker interaction with NvAxin (Lane 1). NvAxin also shows a relatively weaker interaction with Spβ-catenin (compare lanes 2 and 5). Unexpectedly, SpAxin shows a weaker interaction with Nvβ-catenin than with SpAxin (compare lane 4 and lane 5). Sp and Nv Axin bind the SpGSK-3β and NvGSK-3β respectively (Lanes 3 and 6). (B) NvAPC-like and Nvβ-catenin interact strongly in vitro (Lane 2) while NvAPC-like shows weaker but consistent interactions with NvAxin and NvGSK-3β (Lanes 1 and 3). (C) NvAxin-GFP and Nvβ-catenin-mCherry interact in vitro

1470 (Lane 2) as previously shown (Figure 7A, Lane 1), changing the conserved leucine on the
1471 Axin-RGS located βcatBM-like sequence to aspartic acid reduces the in vitro interaction
1472 between NvAxin-GFP and Nvβ-catenin-mCherry (Lane 3) as does the same mutation to
1473 the βcatBM-like sequence towards the C-terminus of NvAxin (Lane 4). Mutating the
1474 leucine to aspartic acid in both NvAxin βcatBM-like sequences completely abolishes the
1475 interaction of NvAxin-GFP with Nvβ-catenin-mCherry (Lane 5).
1476

1477

1478

1479

1480

1481

1482

1483

1484

1485

1486

1487

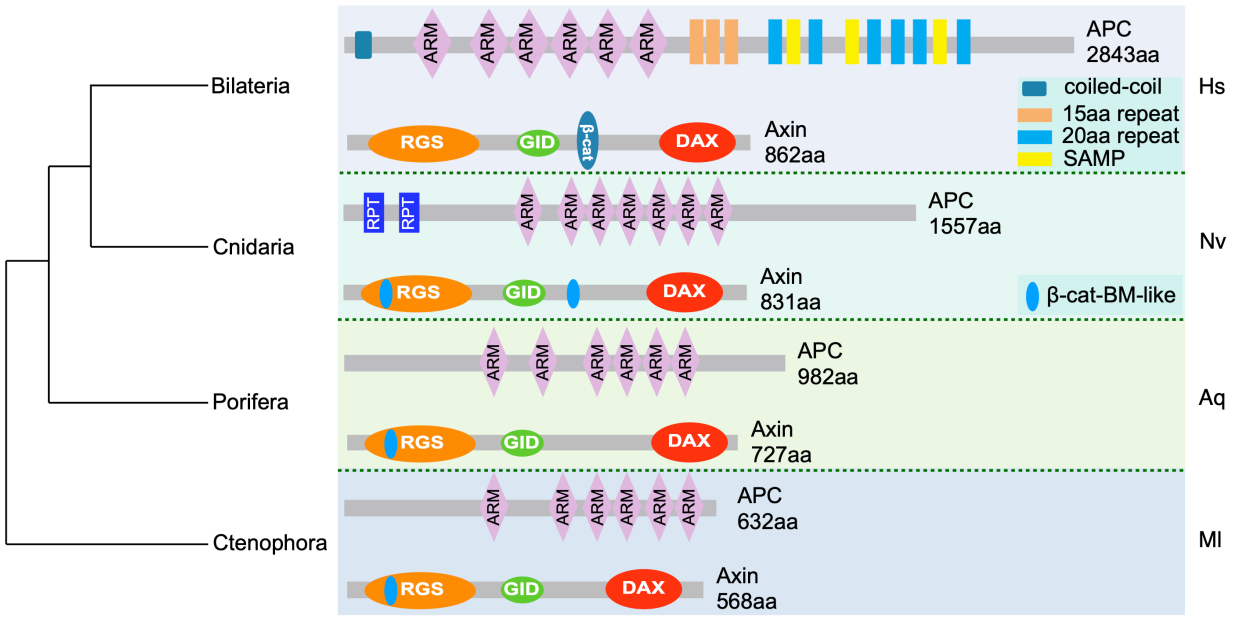

Figure 8- A model for the co-evolution of the β-catenin destruction complex scaffolding proteins Axin and APC-like/APC. The last common ancestor (LCA) to metazoans most likely had an Axin protein that lacked the canonical β-catenin-binding motif (βcatBM) but had a βcatBM-like motif embedded within the RGS domain with possibly promiscuous β-catenin-binding activity. The APC-like protein in this metazoan LCA had ARM domains with strong similarity to APC proteins in extant species. We do not have any evidence that the Axin-APC-like proteins in the metazoan LCA scaffolded a functional β-catenin destruction complex. There were relatively few changes in the main domains in Axin and APC-like in the LCA to the Porifera and later branching metazoans, but there was the acquisition of a critical leucine in the βcatBM-like motif embedded within the RGS domain that may have imparted a higher β-catenin-binding affinity to this motif. Based on the available evidence, we propose that in the Cnidarian-Bilaterian LCA, the βcatBM-like motif embedded within the RGS domain was duplicated with the duplicated copy inserted between the GID and DAX domains of Axin. The Axin and APC-like proteins in this LCA had several protein-protein interactions not reported in bilaterians and as such, may be weak interactions not previously defined in bilaterians that scaffolded a nascent destruction complex. In the Bilateria, the βcatBM on Axin evolved with the acquisition of additional critical amino acids including a critical histidine and the βcatBM-like motif in the RGS domain was lost, possibly through drift. The Axin protein in the Bilateria did not gain additional major domains, but the APC protein gained multiple domains that allowed it to interact strongly with several components of the destruction complex and over 100 other proteins (Nelson and Nathke, 2013). Here, the domains on the bilaterian APC have been simplified for clarity but the additional domains can be seen in Fig. 1D. Model was created using BioRender.

1517 **Supplementary Table 1. The primary protein interaction domains on Axin**
1518 **proteins from bilaterian and non-bilaterian taxa.** In bilaterians (black), Axin
1519 proteins contain APC- (RGS), GSK-3β- (GID), β-catenin- (β-cat), and Disheveled-
1520 (DAX) binding domains. In non-bilaterians (red), the conserved β-catenin binding
1521 domain between the GID and DAX domains is absent.
1522

1523

Species Name & Accession # / Axin Domains	RGS	GID	β-cat	DAX
Strongylocentrotus purpuratus (XP_003729076)	✓	✓	✓	✓
Saccoglossus kowalevskii (NP_001158475)	✓	✓	✓	✓
Platynereis dumerilii (ANS60441)	✓	✓	✓	✓
Crassostrea gigas (EKC24785.1)	✓	?	✓	✓
Branchiostoma floridae (XP_035695674)	✓	✓	✓	✓
Homo sapiens (NP_003493)	✓	✓	✓	✓
Mus musculus (AAC53285)	✓	✓	✓	✓
Xenopus laevis (NP_001081874)	✓	✓	✓	✓
Danio rerio (BAA92439)	✓	✓	✓	✓
Hofstenia miamia (KJ658749.1)	?	✓	✓	✓
Tribolium castaneum (NP_001280495)	✓	?	✓	✓
Drosophila melanogaster (NP_733336)	✓	✓	✓	✓
Apis mellifera (XP_006564444)	✓	✓	✓	✓
Nematostella vectensis (XP_048576223)	✓	✓	×	✓
Mnemiopsis leidyi (ML04208a)	✓	✓	×	✓
Amphimedon queenslandica (NP_001266244)	✓	✓	×	✓
Trichoplax adhaerens (XP_002109778)	✓	✓	×	✓

1524
1525
1526
1527
1528

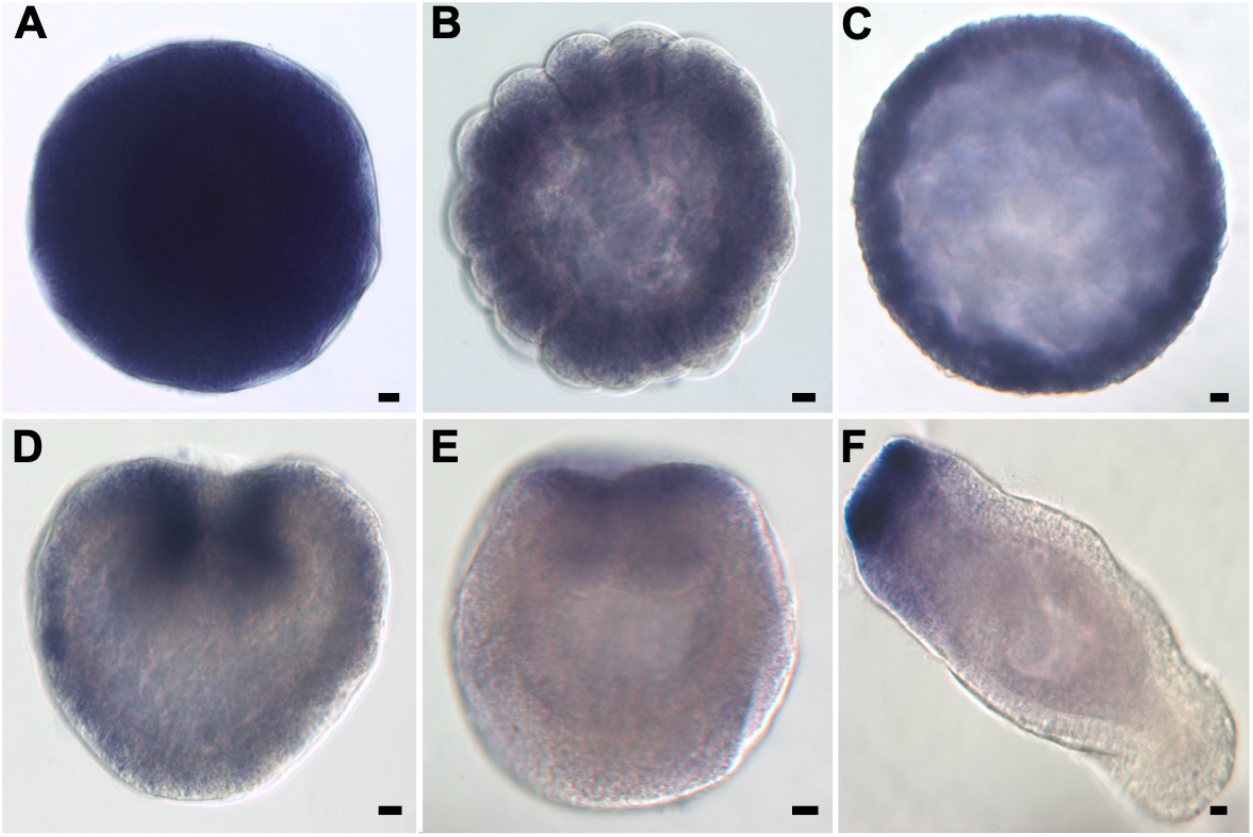

Supplementary Figure 1- Whole mount RNA in situ hybridization shows the expression of *Axin* in *Nematostella* eggs and embryos. Axin is ubiquitously expressed in the egg, and during cleavage and blastula stages (A-C), however Axin is asymmetrically expressed at the animal pole at early and late gastrula stage (D, E) and the oral side at planula stage (F). Scale bar = 10 μm.

1554

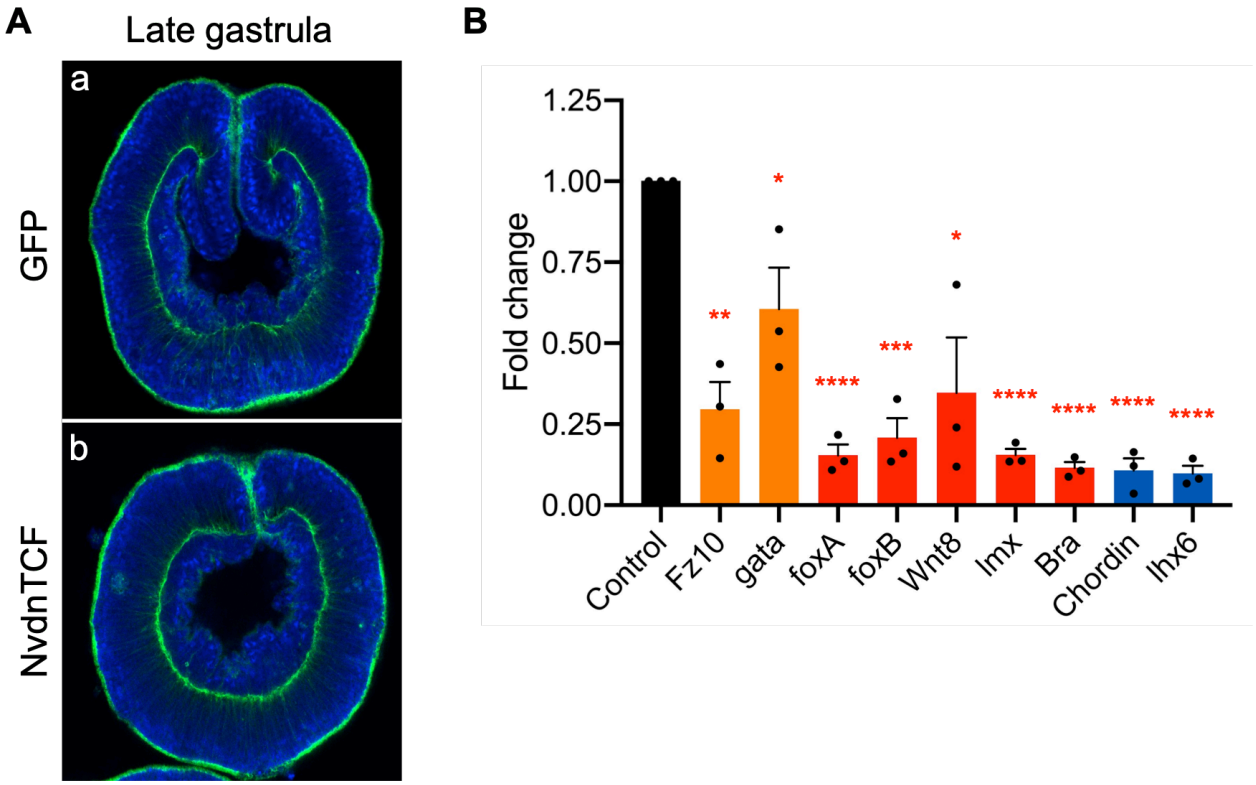

1555
1556
1557 **Supplementary Figure 2-The effect of NvTcf knockdown on primary**
1558 **invagination and endomesodermal and pharyngeal gene expression in**
1559 ***Nematostella* embryos.** (A) Compared to GFP overexpressing control embryos (a),
1560 NvdnTCF-overexpressing embryos (b) initiated primary invagination but failed to
1561 maintain a normal archenteron epithelium at the late gastrula stage. (B) qPCR analysis
1562 of NvdnTCF-overexpressing embryos at 24 hpf (hours post fertilization) showed that all
1563 genes expressed in cells derived from animal pole blastomeres (orange, red, and blue
1564 bars) are downregulated. qPCR experiments were replicated with three separate batches
1565 of embryos with three technical replicates in each experiment. GAPDH was used as the
1566 internal control. Statistical significance was determined using the Unpaired t test. ****,
1567 $p<0.0001$; ***, $p<0.001$; **, $p<0.01$; *, $p<0.05$; n=3.
1568

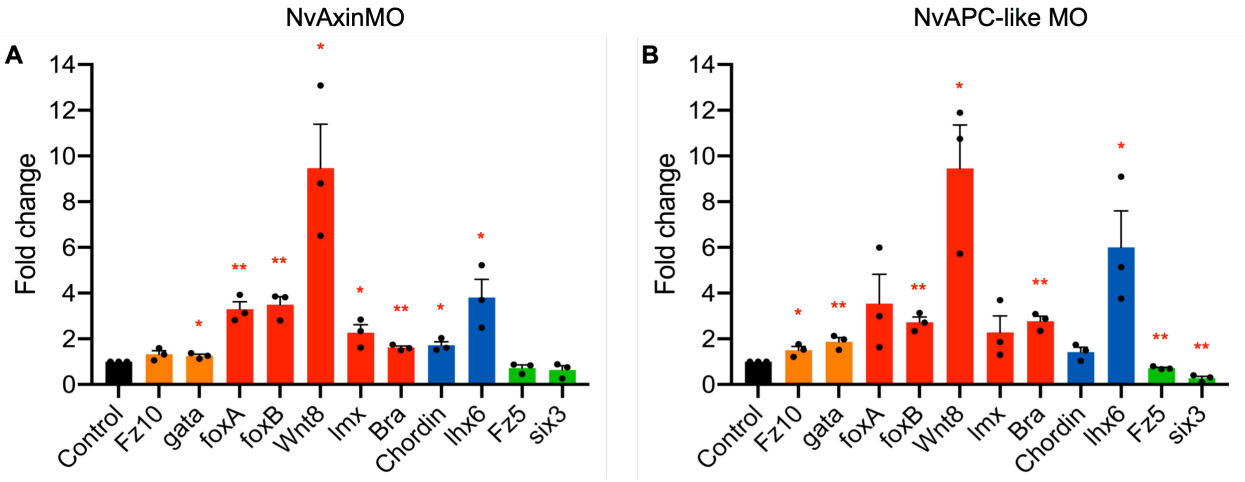

Supplementary Figure 3- Morpholino mediated knockdown of Axin or APC-like upregulates endomesoderm gene expression in *Nematostella* embryos. (A,B) Endomesoderm and pharynx gene markers were upregulated in NvAxinMO or NvAPC-like MO-injected embryos compared to control MO (black bars). The qPCR experiments were replicated with three separate batches of embryos, with three technical replicates in each experiment. GAPDH was used as the internal control. Statistical significance was determined using the Unpaired t test. **, $p<0.01$; *, $p<0.05$; n=3.

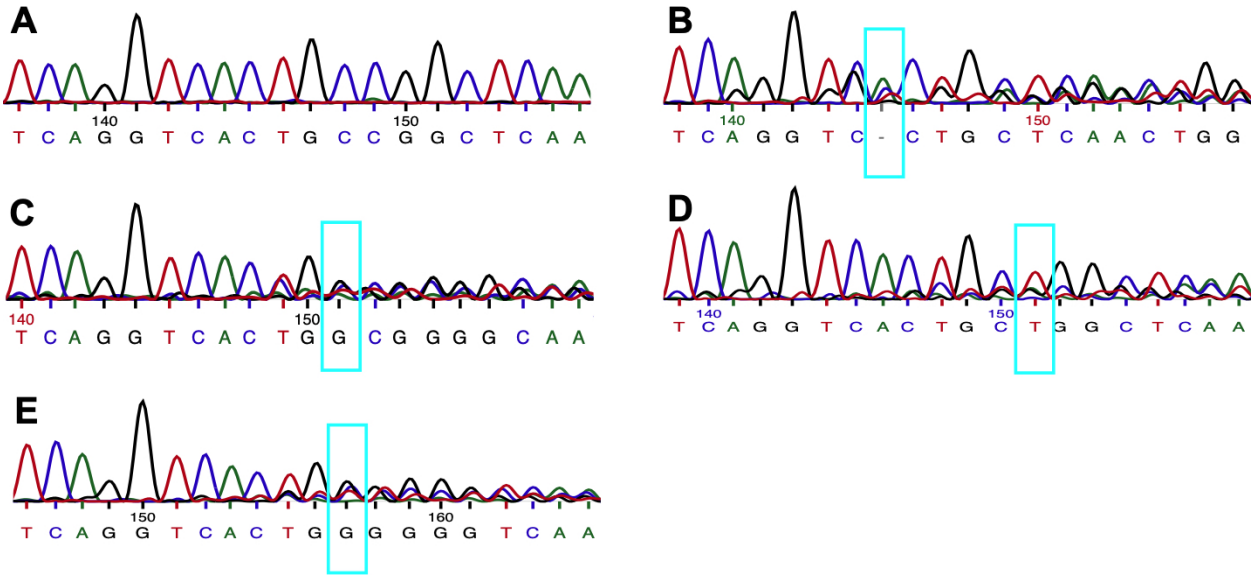

Supplementary Figure 4- Confirmation of successful CRISPR/Cas9-mediated gene editing with Sanger sequencing using a single injected embryo from each group. Compared to the Cas9 only injected embryo (A), the sequencing chromatograms showed that injection of NvAxingRNA/Cas9 induced deletions or mutations (cyan box) at the targeted region of the Axin gene (B-E).

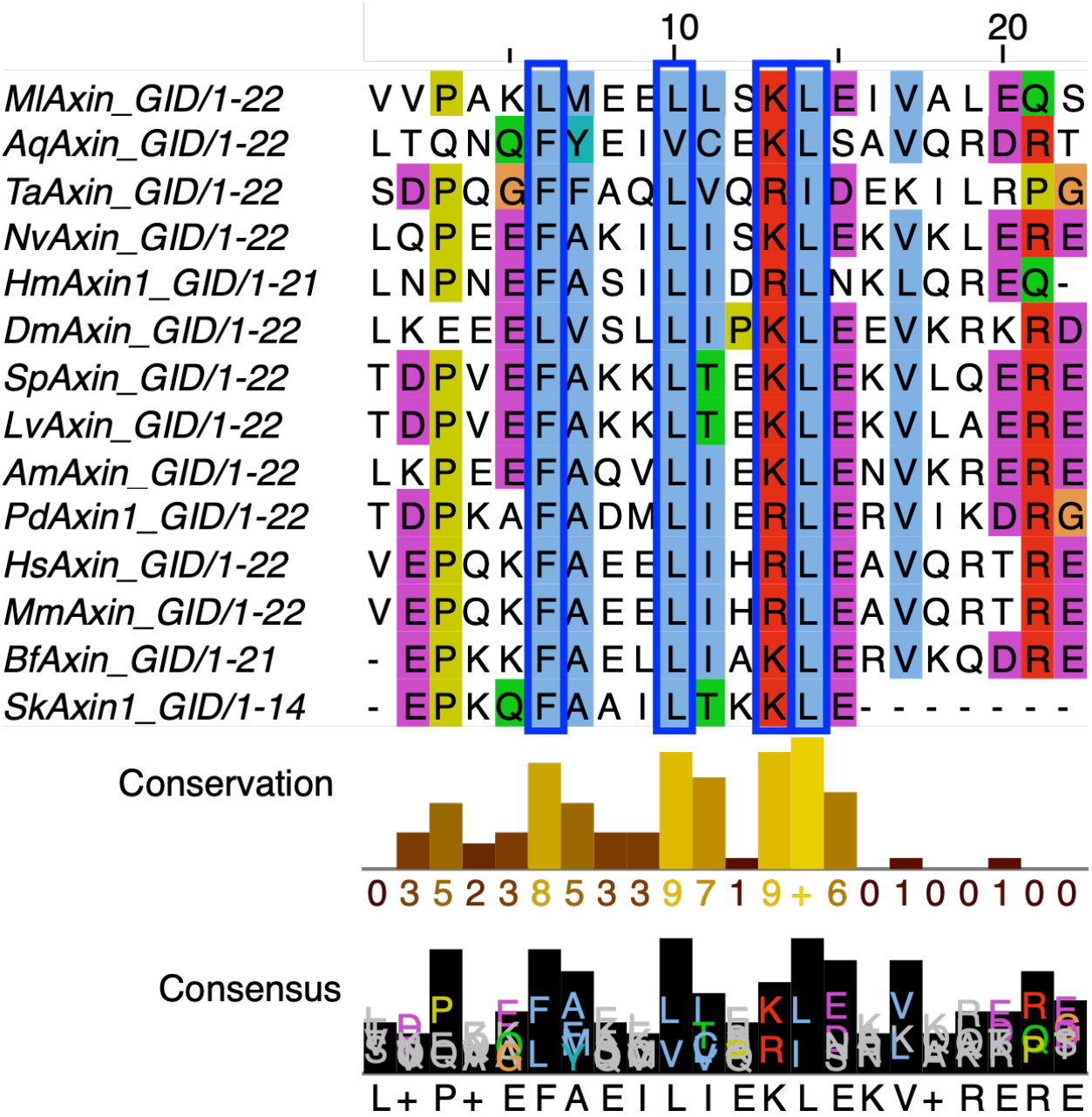

Supplementary Figure 5- The protein sequence alignment of Axin GID domains in various metazoan taxa. The top panel shows the alignments of amino acids sequence using Clustal Omega and Jalview. Conserved amino acids are highlighted in different colors, while gaps are represented in white. The bottom panel is the analysis of conservation and consensus. *Ml*, *Mnemiopsis leidyi*; *Aq*, *Amphimedon queenslandica*; *Ta*, *Trichoplax adhaerens*; *Nv*, *Nematostella vectensis*; *Hm*, *Hofstenia miamia*; *Dm*, *Drosophila melanogaster*; *Sp*, *Strongylocentrotus purpuratus*; *Lv*, *Lytechinus variegatus*; *Am*, *Apis mellifera*; *Pd*, *Platynereis dumerilii*; *Hs*, *Homo sapiens*; *Mm*, *Mus musculus*; *Bf*, *Branchiostoma floridae*; *Sk*, *Saccoglossus kowalevskii*. Blue boxes highlight the critical residues for the interactions between Axin and GSK-3β.

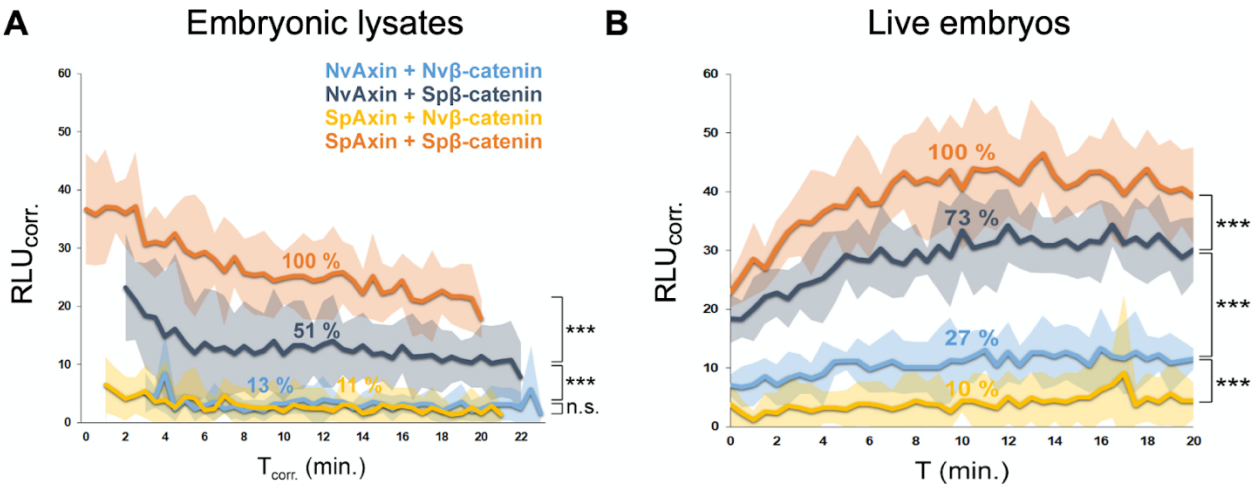

Supplementary Figure 6-The interaction of Nv- and SpAxin with Nv- or Spβ-catenin proteins in *Nematostella* embryos or embryonic lysates. Nv/SpAxin and Nv/Spβ-catenin proteins were fused to click beetle green (CBG) split luciferase fragments, and luciferase activity was detected in embryo lysates (A) and live embryos (B) (n ≈ 150-300 per sample). Axin proteins were labeled C-terminally with the N-terminus of CBG (CBG-N) while β-catenin proteins were labeled N-terminally with the C-terminus of CBG (CBG-C), each connected by a flexible linker peptide. Proximity caused by protein-protein interaction results in complementation of CBG split-luc fragments into functional luciferase and hence stronger luminescence. Plots show moving averages (lines) and 95% confidence intervals (shaded areas) from three independent experiments that represent biological and technical replicates. Percentages are relative intensities compared to a combination of constructs with the strongest signal (SpAxin + Spβ-catenin) averaged across all replicates and timepoints. $RLU_{corr.}$ – intensity of luminescence in relative luciferase units normalized to the amount of expressed protein in each sample (as determined by Nanoluciferase signal). T, T_{corr} – time of measurement (corrected by the delay necessary to lyse embryos) *** $p < 0.001$, n.s. – not significant, Student's t-test.

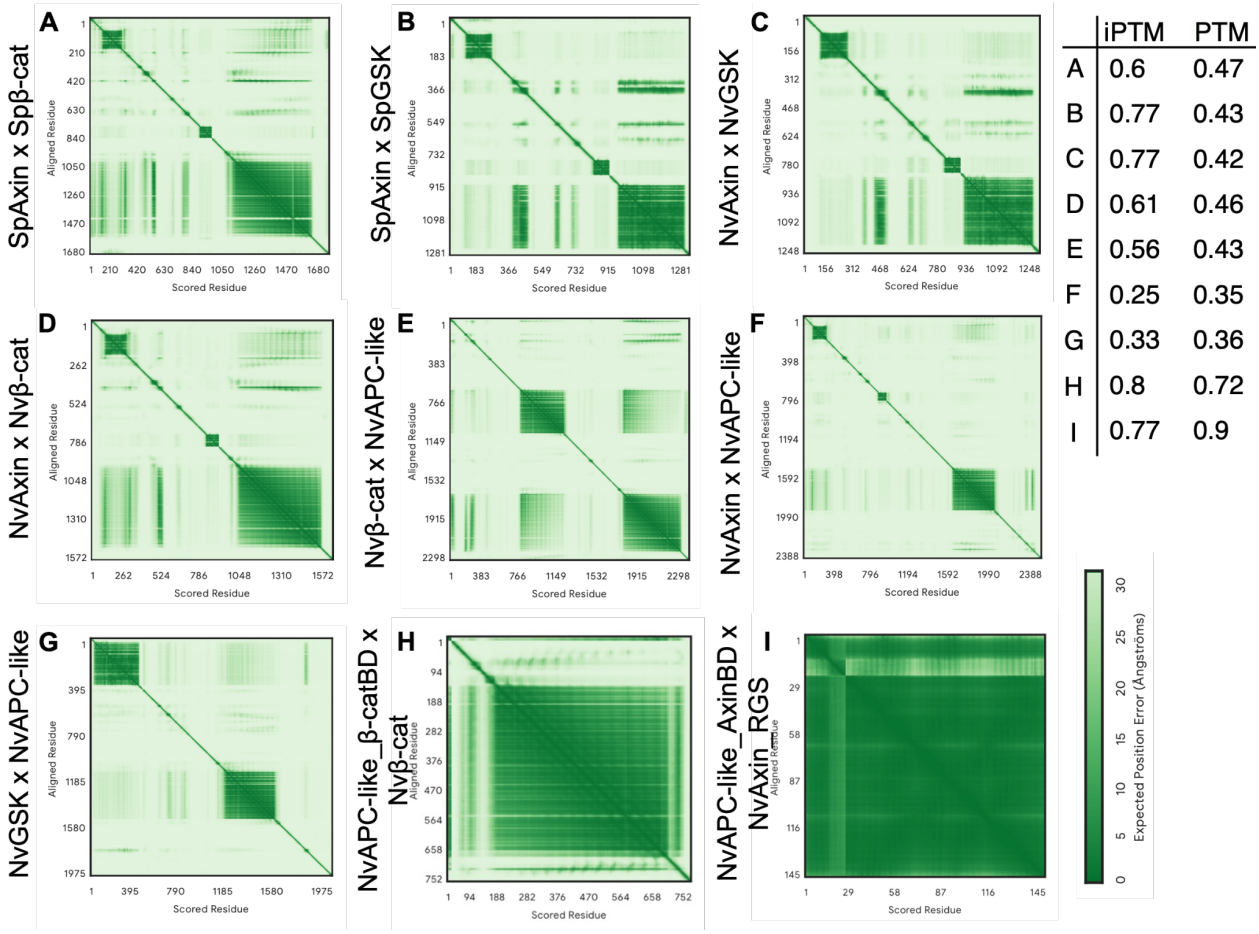

	iPTM	PTM
A	0.6	0.47
B	0.77	0.43
C	0.77	0.42
D	0.61	0.46
E	0.56	0.43
F	0.25	0.35
G	0.33	0.36
H	0.8	0.72
I	0.77	0.9

Supplementary Figure 7- AlphaFold-based predictions of protein-protein interactions between Nvβ-catenin/Spβ-catenin and components of the β-catenin destruction complex. The expected aligned error (PAE) plots for models of interactions between (A) SpAxin and Spβ-catenin (Spβ-cat), (B) SpAxin and SpGSK, (C) NvAxin and NvGSK-3β, (D) NvAxin and Nvβ-cat, (E) Nvβ-cat and NvAPC-like, (F) NvAxin and NvAPC-like, (G) NvGSK-3β and NvAPC-like, (H) NvAPC-like_β-catBD and Nvβ-cat, (I) NvAPC-like Axin binding domain (NvAPC-like_AxinBD) and NvAxin RGS. In the PAE plots, the dark green regions indicate low position error (high confidence in the relative positioning of the interacting residues), whereas light green regions indicate higher positional error (lower confidence). The iPTM and PTM scores, which represent confidence in the predicted inter-protein and intra-protein interactions, are also provided for each model on the right side of figure.

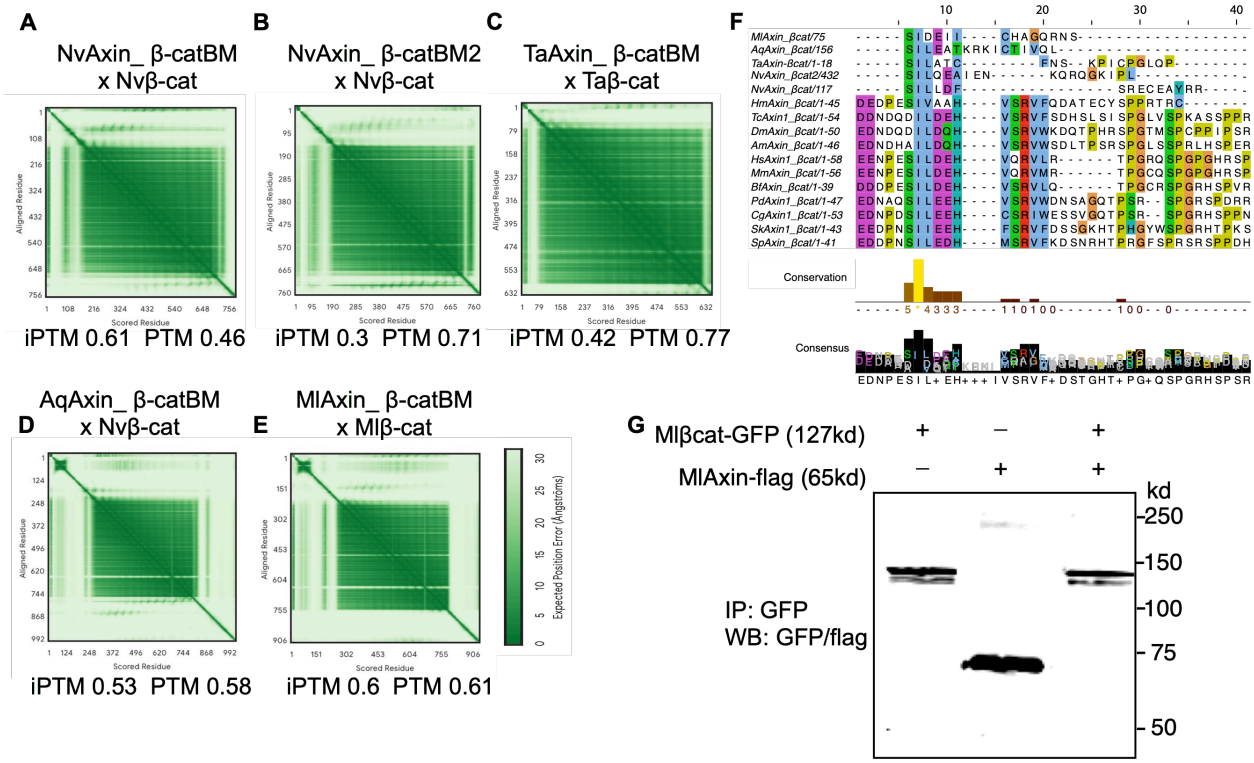

Supplementary Figure 8- Prediction of non-bilaterian Axin-β-catenin binding motif (βcatBM) using AlphaFold 3. (A-E) The Predicted Aligned Error (PAE) plots show the predicted interactions between NvAxin_βcatBM or NvAxin_βcatBM2 (duplicated βcatBM in NvAxin) and Nvβ-catenin, TaAxin_βcatBM and Taβ-catenin, AqAxin_βcatBM and Aqβ-catenin, MlAxin_βcatBM and Mlβ-catenin. In the PAE plot, dark green regions indicate low positional error (high confidence in the relative positioning of the interacting residues), while light green regions indicate higher positional error (lower confidence). The iPTM and PTM scores, which represent confidence in the predicted inter-protein and intra-protein interactions, are also provided for each model. (F) Protein sequence alignments of various bilaterian Axin-βcatBM domains with the predicted NvAxin-βcat, TaAxin-βcat, AqAxin-βcat and MlAxin-βcat motifs. Each residue in the alignment is color-coded, while gaps are shown in white. Conservation and consensus analysis are presented at the bottom of the sequence alignment. Sequence alignments were performed using Clustal Omega and Jalview. (G) An in vitro analysis of *Mnemiopsis* Axin and *Mnemiopsis* β-catenin interaction. Co-IP analysis of MlAxin-Flag and Mlβ-catenin-GFP fail to show an interaction between these two proteins in vitro (lane 3). *Ml*, *Mnemiopsis leidyi*; *Aq*, *Amphimedon queenslandica*; *Ta*, *Trichoplax adhaerens*; *Nv*, *Nematostella vectensis*; *Hm*, *Hofstenia miamia*; *Tc*, *Tribolium castaneum*; *Dm*, *Drosophila melanogaster*; *Am*, *Apis mellifera*; *Hs*, *Homo sapiens*; *Mm*, *Mus musculus*; *Bf*, *Branchiostoma floridae*; *Pd*, *Platynereis dumerilii*; *Cg*, *Crassostrea gigas*; *Sk*, *Saccoglossus kowalevskii*; *Sp*, *Strongylocentrotus purpuratus*.

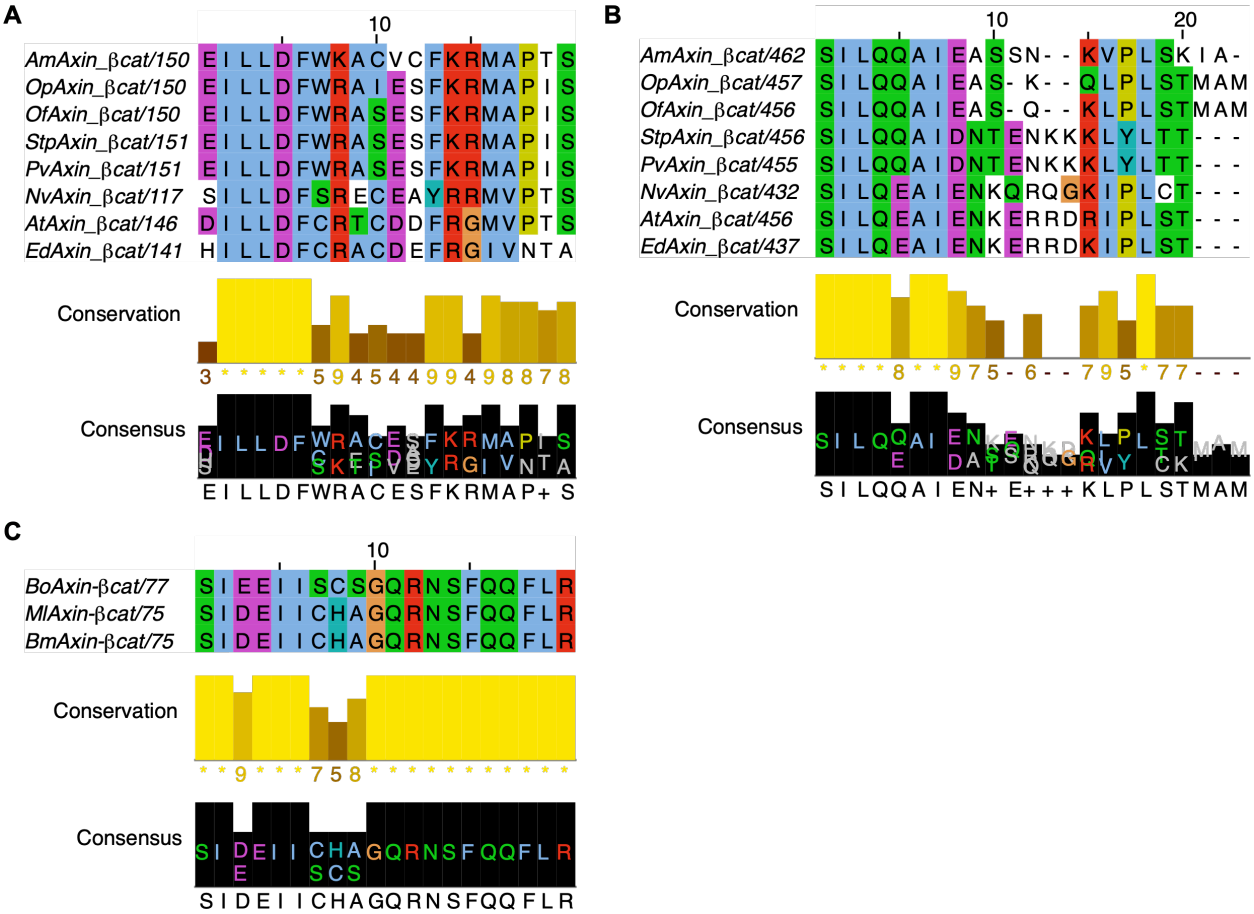

Supplementary Figure 9-The protein sequence alignment of Axin-β-catenin binding motif (βcatBM) -like sequence in cnidarians and ctenophores. The top panels show the alignments of amino acids sequence of βcatBM-like in Axin-RGS (A) or C-terminal (B) generated using Clustal Omega and visualized with Jalview in cnidarian Axins. (C) Similar alignment of the βcatBM-like in Axin-RGS from three ctenophore species. Conserved amino acids are highlighted in distinct colors, while gaps are shown in white. The bottom panels in A, B and C show the analysis of conservation and consensus derived from the alignment. *Nv, Nematostella vectensis; Ed, Exaiptasia diaphana; At, Actinia tenebrosa; Op, Oculina patagonica; Am, Acropora muricata; Stp, Stylophora pistillata; Of, Orbicella faveolata; Pv, Pocillopora verrucosa; Ml, Mnemiopsis leidyi; Bo, Beroe ovata; Bm, Bolinopsis microptera.*